Atmos. Chem. Phys. Discuss., 7, 2389–2475, 2007
www.atmos-chem-phys-discuss.net/7/2389/2007/

Atmospheric Chemistry and Physics Discussions

An overview of the HIBISCUS campaign

J.-P. Pommereau[1], A. Garnier[1], G. Held[2], A.-M. Gomes[2], F. Goutail[1], G. Durry[1,*], F. Borchi[1], A. Hauchecorne[1], N. Montoux[1], P. Cocquerez[3], G. Letrenne[3], F. Vial[4], A. Hertzog[5], B. Legras[4], I. Pisso[4], J. A. Pyle[5], N. R. P. Harris[5], R. L. Jones[5], A. Robinson[5], G. Hansford[5], L. Eden[5], T. Gardiner[6], N. Swann[6], B. Knudsen[7], N. Larsen[7], J. Nielsen[7], T. Christensen[7], F. Cairo[8], M. Pirre[9], V. Marécal[9], N. Huret[9], E. Rivière[9,*], H. Coe[10], D. Grosvenor[10], K. Edvarsen[11], G. Di Donfrancesco[12], P. Ricaud[13], J.-J. Berthelier[14], M. Godefroy[14], E. Seran[14], K. Longo[15], and S. Freitas[15]

[1]CNRS-Service d'Aéronomie, Verrières le Buisson, France
[2]Instituto de Pesquisas Meteorológicas, UNESP, Bauru, Brazil
[3]Centre National d'Etudes Spatiales, Toulouse, France
[4]CNRS-Laboratoire de Météorologie Dynamique, Palaiseau, France
[5]University of Cambridge, Dept of Chemistry, Cambridge, UK
[6]National Physical Laboratory, Teddington, UK
[7]Danish Meteorological Institute, Copenhagen, Denmark
[8]CNR-Institute for Atmospheric Science and Climate, Roma, Italy
[9]CNRS-Laboratoire de Physique et Chime de l'Environment, Orléans, France
[10]University of Manchester Institute of Science and Technology, Manchester, UK
[11]Norwegian Institute for Air Research, Kjeller, Norway
[12]ENEA, Ente Per le Nuevo Tecnologie, l'Energia, l'Ambiante, Roma, Italy
[13]CNRS Laboratoire d'Aérologie, Toulouse, France

[14]CNRS Centre d'Etude des Environnements Terrestre et Planétaires, St Maur, France
[15]CPTEC, Centro de Previsão de Tempo e Estudos Climàticos, Cachoeira Paulista, Brazil
[*]now at: Université de Reims Champagne-Ardenne/CNRS Groupe de Spectrométrie Moléculaire et Atmosphérique, France

Received: 19 January 2007 – Accepted: 9 February 2007 – Published: 21 February 2007

Correspondence to: J.-P. Pommereau (pommereau@aerov.jussieu.fr)

Abstract

HIBISCUS was a field campaign for investigating the impact of deep convection on the Tropical Tropopause Layer (TTL) and the Lower Stratosphere, which took place during the Southern Hemisphere summer in February–March 2004 in the State of São Paulo, Brazil. Its objective was to provide a set of new observational data on meteorology, tracers of horizontal and vertical transport, water vapour, clouds, and chemistry in the tropical UT/LS from balloon observations at local scale over a land convective area, as well as at global scale using circumnavigating long-duration balloons. Overall, the composition of the TTL, the region between 14 and 19 km of intermediate lapse rate between the almost adiabatic upper troposphere and the stable stratosphere, appears highly variable. Tracers and ozone measurements performed at both the local and the global scale indicate a strong quasi-horizontal isentropic exchange with the lowermost mid-latitude stratosphere suggesting that the barrier associated to the tropical jet is highly permeable at these levels in summer. But the project also provides clear indications of strong episodic updraught of cold air, short-lived tracers, low ozone, humidity and ice particles across the lapse rate tropopause at about 15 km, up to 18 or 19 km at 420–440 K potential levels in the lower stratosphere, suggesting that, in contrast to oceanic convection penetrating little the stratosphere, fast daytime developing land convective systems could be a major mechanism in the troposphere-stratosphere exchange at the global scale.

The present overview is meant to provide the background of the project, as well as overall information on the instrumental tools available, on the way they have been used within the highly convective context of the South Atlantic Convergence Zone, and a brief summary of the results, which will be detailed in several other papers of this special issue.

1 Introduction

The tropical Upper Troposphere/Lower Stratosphere (UT/LS) is a key region for both stratospheric ozone depletion and climate. It is the source region of ozone-depleting substances – organic chlorine, bromine and possibly iodine – as well as of long-lived source gases – nitrous oxide, methane –, which after oxidation at high altitude and transport at mid-and high latitude by the Brewer-Dobson circulation, are controlling ozone chemistry. It is also the region controlling the water vapour content of air entering the stratosphere, which is partly responsible for the cooling of the stratosphere. The tropical UT is the altitude level where ozone, an efficient greenhouse gas at this altitude, is found to be highly variable either because of its formation by photochemical precursors lifted by convection, or by quasi-horizontal exchange with the lowermost stratosphere, and finally the region most exposed to NO_x production by lightning within thunderstorms.

There are a number of unresolved issues in the Tropical UT/LS, such as the respective role of large-scale lifting, convective overshooting, radiative heating and gravity waves, in the formation of the cold point tropopause, in the dehydration of air entering the stratosphere and more generally of troposphere-stratosphere exchange

Based on the assumption that the largest vertical motion into the stratosphere is occurring where the temperature of the tropopause is the lowest, Newell and Gould-Stewart (1981) have suggested the idea of a limited region of entry of tropospheric air into the stratosphere, the "Stratospheric Fountain" above Micronesia, also called "the Maritime Continent", in October–March. But, as shown by Danielsen (1993) from ER-2 observations during the STEP mission over Northern Australia in 1987, as well as radiosondes at Darwin and Samoa in the South Pacific (e.g., Danielsen, 1993; Folkins et al., 1999; Gettelman et al., 2002), maritime convection and cyclones result mainly in large-scale lifting and thus cooling of the tropopause, but convection hardly penetrates the stratosphere in those areas. Stratospheric penetration requires systems of extremely large Convective Available Potential Energy (CAPE), named continental-

maritime systems by Danielsen, which only occur over land. They result in a rapid adiabatic vertical transport by overshooting cumulus cloud turrets that becomes irreversible due to entrainment of, and mixing with stratospheric air.

However, convective overshootings are thought to be rare. Convection reaches only the upper troposphere where a barrier to vertical mixing could be generally observed around 14 km, the bottom of the so-called Tropical Tropopause Layer (TTL) (Folkins et al., 1999). The proposal thus made by Sherwood and Dessler (2000) for troposphere-stratosphere exchange (TSE) is a two-step process: a vigorous convective lifting up to the bottom of the TTL followed by a slow ascent after radiative heating in the TTL, a process known as the "mixing layer" hypothesis.

There is only a very limited set of observations over continents because of the many constraints in making in-situ aircraft or balloon observations next to deep convective clouds, and therefore most of observations have been carried out over oceanic areas. The frequency of occurrence and thus the global contribution of stratosphere-penetrating land mesoscale systems is difficult to assess. It is only very recently that comparisons between space-borne radar and Visible-IR imager observations aboard the NASA-TRMM have shown that land convective systems developing in the afternoon were reaching higher altitude levels than maritime systems (Alcala and Dessler, 2002; Novicky and Merchant, 2004; Liu and Zipser, 2005).

The overall objective of the HIBISCUS project was to provide a set of new observational data on meteorology, tracers of horizontal and vertical transport, water vapour, clouds, and chemistry in the tropical UT/LS from balloon observations at local scale over a land convective area, as well as at global scale using circum-navigating long-duration balloons in the summer season for studying the contrast between land and oceans. After several test flights in February 2001 and 2003, the main experiment took place in January–February 2004 at Bauru (22° S, 49° W) in the State of São Paulo in Brazil.

The present overview is meant to provide the background of the project, as well as overall information on the instrumental tools available, on the way they have been

used within the highly convective context of the South Atlantic Convergence Zone, and a brief summary of the results, which will be detailed in several other papers of this special issue.

2 HIBISCUS objectives

Within the global objective of studying the impact of convection on the tropical UT/LS, a number of specific objectives were identified which could be usefully tackled with the available tools.

First objective is the evaluation of meteorological models analyses and re-analyses. Daily temperature and wind fields at the global scale are provided by model analyses, e.g. ECMWF in Europe and NCEP in the US, initialised from surface, radiosonde and satellite observations. Long-term reanalyses, such as ERA40 for ECMWF and NCEP/NCAR for the U.S., have been recently made available with which possible climatic changes, e.g. tropopause height and temperature in the tropics, are being studied. However, a key question is to know the reliability of the information provided by those models in the tropical UTLS, where few radiosondes are available, and when meteorological satellites were at their very early stage. The proposal was to check actual ECMWF and NCEP representations of wind and temperature in the TTL and the lower stratosphere by comparison with long-duration balloon measurements planned during the campaign, as well as with archived data, which could be retrieved from flights performed in the past in the tropics by the CNES and French laboratories.

The second objective was to establish the net vertical transport by deep convection, and the extent to which convective episodes could transport air into the upper troposphere and the lower stratosphere. This was to be addressed by measuring vertical profiles of tracers, e.g., O_3, H_2O, CH_4, CFCs and short-lived species (SLS), whose gradients and absolute concentrations could provide information on transport and mixing, e.g., signature of newly injected tropospheric trace species in the stratosphere. Local measurements of tracers could be made from short-duration balloons by in-situ

methods, whilst mesoscale simulations (RAMS, LEM) were planned to see how well the updraught could be represented in the models and if necessary, adjust the parameterisation.

Next is the meridional exchange. Following Hoskins et al. (1991), the stratosphere could be divided into an "overworld", corresponding to the range of potential temperature where isentropic surfaces above the tropical cold point tropopause at about 380K and a subtropical "lowermost stratosphere" below, connected to the tropical upper troposphere. Global observations from space show that many chemical species have different tropical and extra-tropical mixing ratios along an isentropic surface in the "overworld" lower stratosphere. This indicates the existence of a subtropical barrier with a strong gradient of potential vorticity (PV), but weakening at lower altitude in the tropical stratosphere. The degree of permeability of the barrier and the altitude range where the meridional transport occurs are poorly known and not well represented in meteorological models. Filamentation processes certainly play a role, but horizontal mixing by inertia-gravity waves has also to be considered. The plan was to address those questions by measurements of stratospheric tracers, like ozone and H_2O, at global and local scale, as well horizontal winds from long-duration balloon flights, in combination with the use of a PV contour advection model.

A further objective is the study of meso- and small-scale waves. Waves generated in the troposphere and/or by the jet streams, displace air masses. Much of this displacement is reversible, but the irreversible component leads to the net transport of air. This is particularly important around the tropopause where such a mechanism may inject tropospheric gases, such as CH_4 and H_2O, into the stratosphere and stratospheric ozone into the troposphere. Small-scale processes may also play a role in preventing H_2O reaching the stratosphere. These processes are particularly important near the sub-tropical jet, which acts as a barrier preventing transport of chemical species from low to high latitudes. Larger scale waves also lead to layering and filamentation of air masses in the lower stratosphere, contributing to irreversible mixing. Meteorological instrumentation on board the long-duration balloons should allow the study of both

large- and small-scale dynamical processes. Low frequency (inertial or smaller) waves are detectable from horizontal excursions of constant-level balloons. Higher frequency gravity waves induce vertical motions, which are recorded by pressure and temperature sensors.

Among most important issues in the TTL is the water vapour, which plays a vital role in both chemistry and radiation of the upper troposphere and lower stratosphere. But there are significant uncertainties in the detailed mechanism, which controls H_2O amounts reaching the stratosphere, the amounts present there, and the causes of observed trends.

H_2O can be regarded as a tracer, but it has the added complexity that it can be removed by condensation and sedimentation. Dehydration processes in the tropical tropopause region, which are known to be of crucial importance in controlling the water vapour distribution in the global stratosphere, remain poorly understood in quantitative terms. The original proposal of large-scale ascent leading to cooling and widespread dehydration (Brewer, 1949), refined by Newell and Gould-Stewart (1981) who argued for more localised injection, and by Danielsen (1982 and 1993) who suggested a possible role for overshooting cumulonimbus clouds, has recently been revisited. For example, Pfister et al. (2001) suggested a potential role for dehydration arising from adiabatic cooling due to gravity waves and Dessler (1998) again argues for more widespread ascent and dehydration. Finally, Sherwood and Dessler (2000) suggested the existence of a transition layer in the tropical UT, where dehydration in overshooting cumulonimbus clouds is followed by a general radiatively driven ascent.

The objective within HIBISCUS was to carry out water vapour measurements in the TTL and the lower stratosphere, in-situ over Brazil with tuneable diode laser (TDL) and surface acoustic waves (SAW) methods, as well as remotely all over the tropical belt by vis-near IR solar occultation spectrometry from long-duration balloons.

There are also many open questions in the tropics regarding aerosols and clouds. Their altitude and optical properties are very important for the radiative transfer budget in the atmosphere. Stratified aerosol layers have been observed up to 30 km in this

region, as well as occasional thin sub-cirrus layers of several 100 km of horizontal extension in the upper troposphere. Mechanisms, which keep such cirrus clouds stable for long periods and large spatial extensions, are not completely clear yet. The very limited amount of measurements available on tropical thin and ultra-thin cirrus clouds – as simultaneous measurements of cloud densities, water vapour and temperature – do not justify per se the observed stability of such ice crystal layers. Possible dynamical mechanisms could be addressed to sustain the life of the clouds: like slow upwelling through them and/or slow micro-convection inside the clouds forced by radiation.

The most likely process responsible for this layering is the episodic local injection of aerosol (of possibly different nature) and perhaps ice crystals through the tropopause by the overshooting of deep convective systems, known as "turrets". The objective within HIBISCUS was to measure the vertical distribution of clouds and aerosol, together with water vapour and temperature in the TTL using balloon-borne micro-lidar and backscatter instruments, as well as remotely at global scale with the vis-near IR spectrometer. The measurements were to be interpreted using microphysical, cloud resolving and radiative transfer models.

Another aspect of interest is the chemistry of TTL where short-lived species, such as NO_x, VOC, chlorine, bromine and possibly iodine compounds emitted at the surface, may be injected rapidly into the upper troposphere and perhaps in the lowermost stratosphere also by deep convection. Since these species may be very reactive in the UT/LS, they could have a large impact on stratospheric ozone. However, their presence although suspected, is largely unknown. An important aspect of chemistry in tropical areas is the transformation and partial removal of the species when transported into the convective clouds, as well as heterogeneous conversion in anvils and cirrus, e.g. chlorine activation similar to that observed on Polar Stratospheric Clouds (PSCs) in polar areas, on sub-visible cirrus. The vertical distribution of several important radicals (NO_2, CH_2O, BrO, IO and OClO, if present), as well as ozone potentially formed locally, were to be measured in the upper troposphere and lower stratosphere by remote sensing using a UV-visible spectrometer on board of different type of balloons.

Of particular interest would be the variation of their concentration around the globe to identify the influence of biomass burning, pollution from populated areas and NO_x production by thunderstorms. Chemical changes observed were to be interpreted using 1-D, Lagrangian, mesoscale and global Chemistry-Transport photochemical models.

Finally, is the evaluation of the performances of satellite instruments in the tropical UTLS. A number of remote observations of atmospheric species by space instruments using a variety of techniques is available. However, significant discrepancies are often observed between them in the tropics, where the precision of the retrievals degrades rapidly at decreasing altitude, largely because of the presence of clouds, but also because of increased attenuation, low temperature, interference with water vapour, altitude registration errors, etc. A number of space instruments were expected to be operating during the HIBISCUS period: the long standing NASA SAGE 2 and HALOE, the newer NASA-SAGE 3, the Finland-Canada-France ODIN-OSIRIS and -SMR, and the ESA ENVISAT MIPAS, GOMOS and SCIAMACHY launched in 2002. Unfortunately, the NASA-AURA, planned for 2003, was delayed until May 2004, being after completion of HIBISCUS. The objective in the field was to evaluate their respective performances (altitude registration, precision and accuracy) in the tropical UT/LS of principally ozone, water vapour and NO_2, by comparison with the many profiles anticipated from the long-duration balloon flights.

3 Campaign context

The area chosen for the research was the State of São Paulo in Brazil during the Southern Hemisphere summer, one of the most convectively active regions, known as the South Atlantic Convergence Zone (Fig. 1), where all required local support could be obtained from the Meteorological Research Institute (IPMet) of the São Paulo State University (UNESP).

The region is optimally located to quantify the occurrence of thunderstorms penetrating the tropopause, due to the availability of two S-band weather radars, which

allow to estimate the frequency of radar echoes, at a given reflectivity threshold, penetrating the tropopause. Gomes and Held (2004) studied the echo top (10 dBZ radar reflectivity) distribution of storms during the ten-year period and found that 17% of all storms within the 240 km radar range exceeded 15 km, commonly reaching up to 7–19 km amsl. Figure 2 shows the frequency of days when storms penetrated through the tropopause during February for the 7-year period (1996–2002) of the month of February, in comparison with Febraury 2004. Although it is perceived that the convective activity during the campaign period was slightly below average, the number of days when storm turrets reached the lower stratosphere was amongst the highest in 8 years of observations, viz. 58.6% of the month.

The observational approach in HIBISCUS was based on the use of a combination of balloons of short duration and circumnavigating long-duration balloons, all developed and operated by the Centre National d'Etudes Spatiales (CNES) in France. Their observations were to be complemented by a set of radiosondes, backscatter, ozonesondes and ground-based observations (Doppler radar, lidar, lightning network), largely provided by a Brazilian collaborative project TroCCiBras (Held et al., 2004a, b).

Close collaboration was also set with another EU tropical project TROCCINO$_X$ (Schumann et al., 2007[1]), planning to use the Russian M-55 Geophysica aircraft and the Falcon of the German DLR, based at a nearby airport. Unfortunately, the M-55 could not be available during the HIBISCUS campaign and was only flown the following year, but the Falcon was flown during the main campaign period. Its scientific payload included an upward-looking DIAL Lidar for water vapor and aerosol measurements, a Lyman-alpha detector for water vapor, various instruments to monitor ozone, NO, NO_y, NO_2, CO, CO_2, a CN counter, PCASP-100X and FSSP300 for aerosol measurements, as well as meteorological sensors.

Finally, collaboration was also established with the European Space Agency giving access to the data of ENVISAT instruments prior to their public release and with

[1]Schumann, U., et al.: Tropical Convection, Cirrus and Nitrogen Oxides Experiment (TROCCINO$_X$) Overview, Atmos. Phys. Chem., TROCCINO$_X$, in preparation, 2007.

the ODIN Swedish-Canada-Finish-French satellite for reinforced observations over the area during the period, and finally, with the ozonesonde stations at Samoa, Fiji and Reunion Island for specific ascents during the pass of the long-duration balloons.

3.1 Location

The choice for the campaign was the IPMet facilities in Bauru, 330 km west of the city of São Paulo, in January-March 2004. In addition to its optimum meteorological situation, the station offers the best scientific and operational compromise for carrying out such a demanding programme. North of the subtropical jet in the stratospheric summer easterlies, it allows the flight of short-duration balloons towards accessible areas for safe payload recovery, as well as fast circumnavigating flights of long-duration balloons successively above the SACZ, the South Pacific Convergence Zone (SPCZ) and the ITCZ in the Western Indian Ocean. It offers a suitable balloon launch area, and crucially, a Doppler radar for thunderstorm surveys to detect and avoid showers during launch operations.

3.2 Balloon facility and test flights in 2001–2003

The deployment of such a complex experiment at a relatively new facility (only two short-duration flights in 1997, Pommereau et al., 1999), located in a region prone to thunderstorms during the rainy season, which included the deployment of several new instruments and payloads and the use of a balloon (3SF) for slow overnight descents across the TTL never attempted before, was quite challenging. The testing for the main campaign included a number of flights performed in France in 2001–2003 and at the tropics prior to the main HIBISCUS campaign in 2004. Among these, two test campaigns took place at Bauru during the austral summer 2000–2001 and later in February 2003, the data of which, available in the HIBISCUS database, have been and are currently being used for scientific investigations.

3.2.1 Range and MIR test flights in November 2000 and February 2001

These first test flights were carried at Bauru during the summer 2000–2001. The aims were to test the feasibility (technical, operational and administrative aspects) of MIR flights from Bauru in cooperation with IPMet, as well as the newly developed Inmarsat satellite telemetry. Two initial technical flights were performed in mid-November 2000, lasting for 18 and 19 days before falling over deep convective cells in Northern Australia. The new telemetry performed successfully, but the fall in Australia also showed that it was too heavy for the tropics. Three further flights were attempted in February 2001 where piggyback opportunity was offered for an IR global radiometer, a SAOZ spectrometer and a LABS diode laser. The LABS flight lasted for 49 days, but unfortunately the instrument did not perform properly. The light technical flight carrying the IR radiometer lasted for 71 days and SAOZ-MIR for 39 days providing a unique set of 59 ozone, NO_2 and cloud profiles (Pommereau et al., 2003; Garnier et al., 2005; Borchi et al., 2005). The campaign also offered a first opportunity to study the impact of deep convection on the composition of the upper troposphere by 3-D mesoscale simulations in an extreme storm case, which happened on 8 February 2001 (Held et al., 2003; Marécal et al., 2006; Rivière et al., 2006).

3.2.2 Pre-HIBISCUS/Envisat flights in February 2003

The main objective of this second campaign, funded by ESA and CNES, was a first validation of ENVISAT measurements in the tropics, to which several other objectives were added: instruments and operations testing for HIBISCUS, technical tests of new balloons and payloads and of course science at the tropics. Initially planned for the year before, the campaign was shifted because of the delay to ENVISAT, which was finally launched on 1 March 2002.

In total, seven balloons were flown: 3 of short duration: two ZL type balloons ascending to 30 km and one 3000 m^3 SF type balloon ascending to 22 km only for testing the feasibility of the slow night-time descent across the TTL after the radiative cooling

of the envelope and 4 MIRs. The short-duration balloons were carrying most of the instruments under development for the HIBISCUS campaign: the SAOZ-BrO ultra-violet enhanced version, the SAOZ-H_2O near-IR version, DIRAC N_2O, O_3SSS, H_2O SAW, the micro-lidar, the DIRAC GC, the DESCARTES air sampler (see Sect. 4 for a description of all the HIBISCUS instruments). The payload combination flown on each of them is shown in Table 1.

The MIR were carrying an improved version of the Inmarsat transmitter, a SAOZ-H_2O, and a prototype of the RUMBA H_2O SAW/O_3SSS payload under construction for the constant level flights in 2004. In addition, a number of radiosondes of different types (PTU RS-80, H_2O SAW/O_3 SSS of UCAM) were flown for test purposes in preparation for HIBISCUS. Overall, the short-duration flights and the sondes were very successful providing a large amount of scientific data, as well as useful technical information for improving the instruments. Although two MIR failed, the two MIR-SAOZ flights, including that of the SAOZ new near IR H_2O version, were successful, but the flights were relatively short, only 9 and 10 days, respectively, before falling above hurricanes in the Coral Sea and NW Australia, showing again that a lighter version of the Inmarsat was required for longer duration. Observations performed during these flights have been used for several satellite validation exercises: e.g., SAGE 2 and HALOE ozone (Borchi et al., 2005), ODIN N_2O (Urban et al., 2005), and SCIAMACHY BrO (Sioris et al., 2005; Dorf et al., 2006).

3.3 Collaboration with TroCCiBras

Another decisive advantage was the interest of Brazilian scientists to participate in the project through a number of collaborative observations, as well as in the analysis and interpretation of the data. A scientific collaboration had already been established between the CNRS and IPMet/UNESP in the mid-90's for launching stratospheric balloons from its Bauru Campus and a formal Agreement of Cooperation was signed in 2000. However, resulting from the proposal to bring the EU TROCCINO$_X$ (Tropical Convection, Cirrus and Nitrogen Oxides) project to Brazil during the summer of 2004,

a Brazilian partner project had to be launched, in order to permit the temporary importation and operation of foreign research aircraft, because no such aircraft is allowed to perform measurements in Brazilian airspace, unless invited by and required for a project conducted by Brazilian researchers. Thus, in February 2003, during an International Workshop, IPMet initiated the TroCCiBras (Tropical Convection and Cirrus Brazil) project, inviting all research groups from relevant fields in Brazil to participate. Under the coordination of IPMet and the umbrella of TroCCiBras, HIBISCUS and TROCCINO$_X$ could develop a mutually beneficial scientific collaboration with a number of Brazilian research institutes. An agreement on data exchange, giving access to all HIBISCUS, TROCCINO$_X$ and TroCCiBras scientists to their respective databases, was finalized.

The Brazilian contribution directly relevant to the HIBISCUS project included:

(i) Two Doppler S-band radars at Bauru (BRU) and at Presidente Prudente (PPR, located 240 km west of Bauru in the direction of the balloon flights), extensively used for flight predictions for identifying the presence and location of convective cells and for checking mesoscale and cloud-scale model (RAMS, LEM, MPC) simulations;

Radiosoundings from IPMet performed four times per day for a total of 107, providing a description of convective activity and atmospheric stability during the campaign;

Twice-daily (00:00 and 12:00 UT) runs of the CPTEC Meso-Eta model, centred over Bauru and covering the whole State of São Paulo with a 10×10 km resolution grid, providing 3-hourly forecasts extensively used for flight planning;

Daily 3-D back trajectory calculations from the CPTEC RAMS model for optimising the flights and further analysing their data;

The collection and archiving of the data from the Brazilian radiosonde and automatic weather station networks, three-hourly Meso-Eta model outputs, GOES-E images every half hour, and Brazilian Lightning Detection Network (RINDAT).

A more detailed description of the TroCCiBras Project, its objectives and partner organizations, as well as a summary of the collected data has been provided by Held et al. (2004a, b). In November 2004, an International Workshop was promoted at IPMet, where the research groups participating in the 2004 field campaign were presenting

their preliminary results and discussing future collaboration for joint publications (Held, 2004).

4 Balloon instrumentation, satellites and modelling tools

A number of in-situ and remote sensing instruments have been flown during HIBISCUS on short duration and sounding balloons, and on long-duration platforms. The balloons, their instrumentation, as well as the models to be used were essentially those developed during the 90's for investigating polar ozone depletion in the Arctic (Newman et al., 2002), further adapted to the tropics. The balloon flights were complemented by the use of GOMOS and ODIN satellite observations programmed for reinforced measurements during the period, and a variety of models for the interpretation of their data. They are briefly described below.

4.1 Instrumentation and balloons for mesoscale studies

The list of instruments includes: a grab sampler and a light weight Gas Chromatograph for tracers and short-lived species, two tuneable diode laser payloads for water vapour and methane, a surface acoustic wave (SAW) sensor, a solid state ozone sensor (SSS) and commercial Electro-Chemical ozonesondes, a SAOZ UV-visible spectrometer for remote ozone and NO_2 profile measurements and an extended UV version for BrO, a UV radiometer for photolysis rates, a backscatter diode laser and a backscatter sonde for in situ and a micro-lidar for remote aerosols and clouds observations, an electric field probe and an optical lightning sensor. Depending on scientific objectives and logistical constraints, they were combined in a series of different payloads and flown on a variety of balloon types: (i) Zodiac light (ZL) of 10 000 m^3 volume carrying 120 kg for an ascent up to 30 km, followed by a short float of 1–2 h, e.g. for solar occultation measurements, and a fast descent below a parachute; (ii) Zodiac 3SF (3000 m^3) balloons carrying 150 kg at 21 km, for descending slowly after sunset after the cooling of the en-

velope, used for in situ measurements across the TTL; and (iii) Raven plastic balloons of 240 and 1500 m^3 for soundings.

4.1.1 DIRAC gas chromatograph

DIRAC (Determination In situ by Rapid Analytical Chromatography) is a lightweight gas chromatograph for use on stratospheric balloons developed by the University of Cambridge. The operation and performance of DIRAC are described by Robinson et al. (2000). The overall instrument weight including the flight housing and battery power for an 8-h flight is 30 kg. DIRAC uses a Carboxen adsorbent to pre-concentrate samples of known volume before injection onto a separation column and electron capture detector. It measures a range of halocarbons at a time resolution, which can be adjusted depending on the type of flight being made. For instance, CFC-11 and CFC-113 can be measured at 100-s intervals (0.3–0.7 km resolution depending on balloon vertical velocity) or CFC-11, CFC-113, $CHCl_3$, CH_3CCl_3 and CCl_4 can be measured at 200-second intervals (0.6–1.4 km resolution). It has been successfully deployed on 10 balloon flights including 4 flights during THESEO 1999/2000. The repeatability of standard gas measurements during flight (1 sigma in-flight precision) is 6.5% for CFC-11, 7.5% for CCl_4, 10% for CH_3CCl_3 and 15% for $CHCl_3$.

4.1.2 DESCARTES grab sampler

The tracer instrument DESCARTES (Détermination et Séparation par Chromatographie lors de l'Analyse des Résultats des Traceurs Echantillonnés dans la Stratosphère) is a lightweight (17 kg) balloon-borne grab sampler, developed by the University of Cambridge, in which known volumes of stratospheric air are trapped on sample tubes containing Carboxen. A range of trapped halocarbons (typically 10 compounds) is subsequently measured in the laboratory using a gas chromatograph and electron capture detector. The instrument carries 16 adsorbent tubes, which limits the number of samples, which can be taken per flight. For a detailed discussion see Danis et al. (2000).

It has been successfully deployed on over 20 flights since 1995. The measurement precision (1 sigma) is 3% for CFC-11, 1.5 % for CFC-113, 16% for CCl_4, 5.5% for CH_3CCl_3 and 6.5% for $CHCl_3$.

4.1.3 μSDLA tuneable laser

The micro-SDLA sensor of CNRS-SA is a balloon-borne diode laser spectrometer devoted to the in situ measurement of H_2O, CH_4 and CO_2 in the UTLS by infrared absorption spectroscopy (Durry et al., 2004). Three near-infrared telecommunication-type InGaAs laser diodes are connected by means of optical fibers to an open multipath optical cell providing an absorption path-length of 28 m. The laser beam is absorbed by ambient gas molecules as it is bouncing back and forth between the cell mirrors. CH_4 is monitored at 1.65 μm, CO_2 at 1.60 μm and H_2O at 1.39 μm using a differential detection technique. The payload also includes pressure and temperature sensors. An accuracy of 5% is achieved for a measurement time of 160 ms. The μSDLA sensor was flown twice during HIBISCUS, first on SF2 (sampling rate of one concentration data per second), and then on SF4 (sampling rate of four concentration data per second). To avoid contamination by outgassing from the balloon or the payload only data recorded during the slow night-time descent of the balloons are considered in the TTL and the UT, continued by those during parachute descent in the lower troposphere. Additional tropospheric measurements were also obtained during the ascent in SF2.

4.1.4 TDLAS tuneable laser

The lightweight NPL instrument uses near-infrared tunable diode lasers and an astigmatic Herriott cell to measure spectroscopic absorption over a pathlength of up to 101 m. The instrument has been used for fast response measurements of atmospheric tracers on board balloons (van Aalst et al., 2004) and aircraft (Bradshaw et al., 2002). The instrument was configured for water vapour measurements during the HIBISCUS campaign, using an all-metal gondola designed to minimise out-gassing. The mea-

surements were made at a frequency of 0.7 Hz over three water vapour absorption lines around 1.36 μm which had a range of linestrengths to cover the wide atmospheric concentration range. Analysis was carried out using parameters from the Hitran 2004 Spectroscopic database, and the results had an estimated uncertainty of 10%, with a detection limit of 0.5 ppm.

4.1.5 Surface Acoustic Wave (SAW) H_2O sensor

Frost point hygrometry is a well-established measurement method, with most current instruments using a cooled mirror with an optical source and detector as the sensing element. The instrument of the University of Cambridge is based on this method, but uses a surface acoustic wave (SAW) crystal instead for detection (Hansford et al. 2006). A key advantage of the frost point approach is that it has a calibration based on fundamental relations. The advantage of the SAW method is that fewer monolayers can be detected, therefore being intrinsically more sensitive and has a much faster response relative to a standard mirror frost point hygrometer. An alternating voltage across interdigital electrodes on the surface of the SAW crystal causes oscillations at a well-defined frequency (typically 100 s of MHz). The SAW crystal is placed, together with an accurate platinum resistance thermometer, onto a Peltier cooler. When cooled to the frost point, water vapour condenses onto the SAW surface, reducing the SAW oscillation frequency and amplitude, forming the basis of a feedback circuit. The temperature at which condensation occurs is then related to the ambient water vapour amount. A prototype, weighing less than 3 kg has been flown on several occasions, measuring frost points below –80°C.

4.1.6 Solid State Ozone Sensor (SSS O_3)

The sensor, based on a commercial sensing element, also developed by the University of Cambridge, consists of a thin metal oxide (tungsten oxide) layer mounted on a small (2 mm×2 mm) ceramic tile (Hansford et al., 2005). The principle of operation is that

when heated to its operating temperature, oxygen vacancies, formed thermally at the oxide surface, create electron donor states, resulting in an increase in charge carrier concentration (i.e., a reduction in resistance). O_3 molecules react on the oxide surface filling the oxygen vacancies, decreasing the charge carrier concentration. The resulting increase in electrical resistance, which can be related to O_3 concentration, is then measured. The device has sensitivity to better than 3×10^{10} molecules/cm^3, corresponding to 0.03 ppmv at 50 hPa. The typical time response of the device is in the order of a few seconds. Its weight is less than 0.5 kg, excluding batteries. The particular advantage of this device is that, unlike a conventional ECC sonde, it can operate for several months without intervention.

4.1.7 SAOZ UV-Visible spectrometer

SAOZ is a UV-Vis spectrometer for remote measurement by solar occultation during the ascent of the balloon in the late afternoon and at sunset or sunrise from float altitude. Three versions have been deployed during HIBISCUS: the basic SAOZ in the 300–650 mm spectral region for O_3 (2% accuracy), NO_2 (5%), and cloud extinction (Pommereau and Piquard, 1994), and a UV enhanced version in the 300–400 nm range, SAOZ-BrO, for BrO (15%) (Pundt et al., 2002) and a newly developed 400–1000 nm version for the measurement of H_2O in addition to O_3 and NO_2. The SAOZ payload weighs 18 kg.

4.1.8 NILUCUBE UV radiometer

A new version of the NILUCUBE instrument described by Kylling et al. (2003) was developed for the HIBISCUS campaign. The new NILUCUBE has six channels in each of its six heads. The heads are mounted on the faces of a cube. For each head UV radiation is measured at 312 and 340 nm, with a bandwidth of 10 nm at FWHM. In addition to radiation measurements, the new NILUCUBE includes a GPS for position and timing information, and a magnetic compass for tilt, roll and heading information. The

instrument is not temperature stabilized, in order to save weight. However, temperature is measured for each of the six heads. Data from all sources are sampled every second. The weight of the instrument, including a separate data logging unit, is about 6 kg. Each head measures the irradiance. The new NILUCUBE has improved input optics which deviates less than 5% from the ideal cosine response for zenith angles smaller than 85°. By combining the measurements from all heads, the actinic flux may be deduced, as shown by Kylling et al. (2003).

4.1.9 LABS backscatter diode laser

This instrument developed by CNR-ISAC and ENEA provides an in-situ measurement of the aerosol volume backscatter coefficient and aerosol depolarization at 532 nm. The aerosol volume backscatter coefficient detects the presence of aerosols in the air mass sampled, as well as a rough estimation of their quantity. The aerosol depolarization, being the ratio to what extent the main polarization of the laser is preserved in the backscattering process, gives information on the shape of the sampled aerosols, and in some cases a coarse estimation of their dimensions as well (Buontempo et al., 2006).

4.1.10 Micro-lidar

This lightweight low-power lidar of ENEA and CNR-ISAC employs a miniaturized Nd-YAG pulsed laser firing at 532 nm and is able to give profiles of aerosol backscatter and depolarization during night time, from the altitude of the payload downward to the ground, with a vertical resolution of 30 m and a time resolution of 60 s. In daylight conditions, the system was unable to profile, but operated as a near-range backscattersonde, providing values of backscatter and depolarization at a few tens of metres from its platform. The parameters obtained by MULID observations are, apart from intensity profile and depolarization profile of the backscattered signal, also the extinction profile in optically thin clouds and the cloud top height for optically thick clouds (Di

Donfrancesco et al., 2006).

4.1.11 Lightweight scattering probe

This instrument of the University of Manchester was designed to measure the number size distribution of aerosol particles in the size range 0.3 to 3 μm diameter using light scattering. The instrument uses a white light source and measures the scattered light intensity at 45 and 90 degrees scattering angle, using dual detectors. One of each of the pair of detectors is fitted with a polarising filter to obtain information on particle shape. HIBISCUS provided the first test for this instrument and whilst it flew during the experiment, a critical failure occurred and no data could be retrieved.

4.1.12 AIRS electric field probe

The AIRS electric field instrument of CNRS-CETP is designed to measure the vertical component of the atmospheric electric field from DC to 10 kHz and the electric conductivity of the atmosphere through the relaxation technique. It uses the double probe technique with 2 carbon coated cylindrical electrodes, 3 cm in diameter and 15 cm long, installed at the ends of a vertical boom, 1 m in length, located 25 cm away from the gondola. Grounded plates, also coated with carbon, are installed on the sides of the gondola. They provide a good electrical contact between the electronics ground and the local ionized atmosphere and avoid the detrimental influence of spurious potentials that may arise on the external insulating material of the gondola. High impedance, very low leakage current preamplifiers allow to perform measurements in the low conductivity atmosphere down to a few kilometre altitudes. Data are recorded in 2 channels, one for large amplitude signals, up to ±200 V/m, from DC to ∼2 kHz with a resolution of 4 mV/m and the second one for low amplitude AC signals from ∼5 Hz to 10 kHz with a sensitivity of ∼2 to 3μV/m.Hz$^{1/2}$.

4.1.13 Lightning optical sensor

This sensor developed by CNRS-SA is an attempt to detect lightning and blue-jets flashes from the electric probe. The sensors are made of two photodiodes and amplifiers mounted on the AIRS instrument, the first looking downward within a 180° FOV and the second upward within a 30–80° annular FOV to avoid reflection of lightning flashes on the balloon or pieces of the payload.

4.1.14 Backscatter and ozonesondes

The sondes operated by the Danish Meteorological Institute make use of a Wyoming backscatter sonde (Rosen and Kjome, 1991) made of a Xenon lamp, which emits a white flash every 7 s. The light is scattered by particles and molecules in front of the sonde, and monitored with two photodiodes at 480 and 940 nm, respectively. Two parameters are calculated from this signal: the backscatter ratio (BR), i.e. the ratio between particle and molecule backscatter, and the color index, defined as (BR940/BR480). The color index is correlated with the particle size. An ozone sonde (Electro Chemical Cell), was mounted on the backscatter sonde providing in situ ozone density measurements

4.2 Instrumentation and balloons for global-scale studies

Two types of long-duration balloons are currently available at CNES that have been used for the HIBISCUS investigations: (i) constant level 8.5 m and 10 m diameter superpressure balloons (SPB) carrying 20 kg at 18 and 19 km; and (ii) Infra-Red Montgolfier (MIR) carrying 60 kg at 28 km during daytime and 20–24 km at night.

The choice of instruments for long-duration balloon flights is limited by weight and telemetry capacities of the platforms, as well as the technical maturity of the payloads

4.2.1 SPB instrumentation

The scientific payload on SBP flights designed by CNRS-LMD, called Rumba, carries a GPS for location (±10 m) and horizontal wind calculation (±0.01 m/s), a pressure (±0.6 Pa) and two temperature sensors (±0.25 K at night, 0.3 K during daytime). The data are sampled every 15 min and transmitted via the ARGOS telecommunication system. The temperature sensors are small thermistors (YSI microbeads), mounted 180° apart on a 1-m boom, hanging 5 m below the gondola. The gondola is designed for carrying small passenger instruments. In the present case, they were of two types: a combination of O_3SSS and SAW sensors on the balloons flying at 18 km near the cold point tropopause and a prototype of turbulence sensor designed by CNRS-LMD on those flying at 19 km. The O_3SSS and SAW are essentially identical to those flown on the short-duration balloons, though the operational methods were tailored to the constraints of the long-duration flights. The turbulence sensor is made of a micro-accelerometer (10^{-6} g resolution) sampled at high frequency (200 Hz) measuring the motion of the gondola induced by atmospheric turbulence. The variance in several spectral bands between 0 and 100 Hz is transmitted to the ground.

4.2.2 MIR instrumentation

Depending on the flight, the MIRs were carrying one or two payloads: a service gondola (CNES) controlling the flight (Inmarsat telemetry and remote control) hosting a micro-lidar of ENEA, or the service payload alone and an independent SAOZ payload 40 m below. The micro-lidar was very similar to those flown on short duration balloons, but activated every 15 min during night-time for an average backscatter and depolarization profile below the balloon. The SAOZ long-duration version is also similar to the short-duration version, but with two important differences: the spectral range 400–1000 nm is extended toward the near IR for the measurement of stratospheric water vapour around 760 and 940 nm and O_2 (temperature) around 780 nm; and on-board spectral analyses are carried out because of the strong limitation of telemetry capacity of the

ARGOS system used. Indeed, only the results of the analysis (slant columns and fitting errors) are transmitted whilst the spectra are stored on board in memory for an eventual recovery at the end of the flight.

All service payloads were also carrying a GPS, a pressure sensor and two thermistors, as well as a lightweight (160 g) global IR radiometer developed by CNRS-SA following a design proposed Suomi and Kuhn (1958). The SAOZ payload was also equipped with a GPS, Vaisala RS80 pressure and temperature sensors and two small optical detectors oriented respectively towards nadir for the detection of lightning flashes and zenith for blue-jets.

4.3 Satellites

Two satellite instruments were associated with HIBISCUS for the validation of their measurements in the tropics, and for the scientific exploitation of their validated data in combination with those of the balloons: GOMOS-ENVISAT for ozone and water vapour, and the ODIN-Sub-Millimeter Radiometer (SMR) instrument for N_2O. Their operating modes were oriented toward enhanced observations around the southern tropics during the period of the balloon flights.

4.4 Modelling tools

The interpretation of the large amount of observations collected during the experimental period required the use of modelling tools of different types. These include the ECMWF (Rabier et al., 2000) and the long-term ERA40 (Simmons and Gibson, 2000) and NCEP/NCAR (Kistler et al., 2000) re-analyses, the MIMOSA high-resolution contour advection model (Hauchecorne et al., 2002), the p-TOMCAT CTM (O'Connor et al., 2005), the REPROBUS CTM stratospheric photochemical model (Lefèvre et al., 1994), a mesoscale RAMS regional model (Pielke et al., 1992) and its Brazilian developments on the Regional Atmospheric Modelling System (BRAMS) version (Freitas et

al., 2007[2]) coupled with 3-D back trajectory calculations at mesoscale (Freitas et al., 2000), the MiPLaSMO Lagrangian photochemical model (Rivière et al., 2003), the Microphysical Cloud Model of the Danish Meteorological Institute, the UK Met Office LEM Cloud Resolving Model (Shutts and Gray, 1994; Swann 1998), and finally, the radiative transfer model of NILU. Their use in the interpretation of the HIBISCUS observations will be detailed with the results.

5 The HIBISCUS field campaign

The campaign started on 20 January and ended on 6 March 2004. In total, 18 balloons (6 short and 12 long duration) were flown along with 15 small plastic balloon sondes (10 BKS/O_3, 3 ozonesondes and 2 NILUCUBE). Most disappointing in reference to the plan, was the cancellation of the Geophysica aircraft for which 4 specific balloon flights were planned. They were replaced by coordinated flights with the Falcon, though of course, the measurements could not be performed at the same altitude.

The balloons, the instruments carried by each of them, their performance in flight, as well as the data, which could be expected from each, are summarized in the following section.

5.1 Short-duration balloons and sondes for mesoscale studies

The objective was the study of transport, water vapour, chemistry, cirrus clouds and electric fields associated with convective cells in collaboration with TROCCINO$_X$ aircraft and ground-based measurements carried out by TroCCiBras.

[2]Freitas, S. R. , Longo, K. M. , Silva Dias, M. A. F., Chatfield, R., Silva Dias, P. L., Artaxo, P., Grell, G., Andreae, M. O., Fazenda, A., Rodrigues, L. F., and Panetta, J.: The Coupled Aerosol and Tracer Transport model to the Brazilian developments on the Regional Atmospheric Modeling System. 1: model description and evaluation, Atmos. Chem. Phys. Discuss., in preparation, 2007.

Figure 3 shows the evolution of the meteorology during the campaign and the dates of the balloon flights and sonde ascents. Though the summer season is on average very convective in Southeast Brazil, the ECMWF 6-hourly analysis temperature profiles above the station exhibit large variations. Convective periods display a relatively warm troposphere and a cooler TTL, while low or non-convective periods are marked by a cooler troposphere and a warmer TTL. The altitude difference between 340 and 370 K potential temperature levels is a good indicator of convection. The numbering of the balloon flights corresponds to instrument combinations prepared in advance, which for various reasons could not be followed as expected. Meteorological radiosondes were made four times per day between 5–21 February, otherwise as shown in Fig. 3. The radars were operated permanently during the whole campaign. Table 2 provides the list of instruments flown on each balloon.

5.1.1 ZL balloon flights

The ZLs were used for in-situ measurements of aerosol (LABS) or N_2O (DIRAC) during the ascent/descent of the balloon, together with O_3, NO_2, BrO profile measurements by solar occultation during ascent and sunset period from float altitude, using both the regular SAOZ spectrometer and its UV extended version. Two flights were carried out, one on 31 January (ZL2) at 17:30 LT and the other on 5 February (ZL1) at 17:00 LT. Unfortunately, the DIRAC payload on ZL2 hit the ground during launch operation. Therefore no N_2O profile was available in 2004 (but was in 2003). All other instruments performed well. The two flights were performed over the SACZ, with ZL2 being flown in conditions almost unaffected by nearby convection (Fig. 4, left), but the second (ZL1) during a much more active period, with an intense mesoscale convective system (MCS) of some 300 km extent, about 150 km to the south and south-west of its flight trajectory, as shown by the radar image (Fig. 4, right) and therefore a cooler TTL (minimum temperature of –85°C, instead of –77°C). Clouds were reported up to 12 km by both LABS and SAOZ on 31 January. Higher clouds were seen by SAOZ on 5 February when the atmosphere became totally opaque below 16.5 km in the direction

of the sun at sunset. Relatively strong lightning activity was reported by the RINDAT network, peaking in both cases at some 200 flashes per hour in a 1°×1° area around 18:00 LT near Bauru.

5.1.2 SF Balloon flights

Launched in the late afternoon, these balloons are left descending very slowly (0.5 m/s or less) after their cooling at night, for exploring the TTL and the UT down to 12–14 km. The idea, tested first in 2003, proved to be excellent. Four flights were performed, with all four having slow descents of 3 to 5 h.

In all cases, they were carrying a tuneable diode laser of CNRS-SA or NPL, one or two SAW hygrometers of UCAM, a tracer measuring instrument (the UCAM DIRAC GC or the DESCARTES sampler) and a cloud detecting system (LABS of CNR-ISAC or the ENEA micro-lidar). In addition, they were all carrying an O_3 high-resolution SSS sensor. Finally, the electric field instrument of CNRS-CETP was flown together with the lightning optical sensors. In addition, as shown in Fig. 3, all SF flights were accompanied by backscatter and/or ozonesondes, launched around 22:00 LT in the evening, because of the daytime restriction of the optical measurements. Two noontime NILUCUBE flights were performed during the period, the first, on 13 February in almost cloud-free conditions and the second, on 25 February, on a more convectively active day, when high-altitude clouds where developing around noon.

SF-2 flight

The first balloon, named SF2, was launched on 13 February at 17:18 h LT some 300 km east of a strong convective region over the west of the State of São Paulo, Mato Grosso do Sul and Paraguay (Fig. 5). The balloon reached an altitude of 20 km just before sunset, followed by a 3-h nighttime descent down to 11.8 km, where it was cut down 90 km north of Bauru. From 11:00 LT (14:00 UT) on that day, convective systems began developing in the southeastern quadrant of the Bauru radar, rapidly intensifying

during the early afternoon, later also in the southwest sector and east north east of the radar. At the time of the launch, the nearest storm was about 60–70 km south-east of BRU, but remained more or less stationary and at no stage did it impact on the flight trajectory. However, at the same time, the PPR radar showed a large area of instability moving in from northwest and west, but it never came closer than 300 km from the balloon track (Fig. 6). Towards the end of the flight, some very small (5–10 km) cells appeared just west of the floating balloon, but their tops stayed well below 10 km. The radiosonde profile displays a fast change in lapse rate at 14 km, sometimes called secondary tropopause, a minimum temperature of –75.2°C at 15.7 km (115 hPa, 367 K), topped by an almost isothermal layer reaching up to 20 km. Tropospheric winds were from south-westerly directions up to 15–16 km, originating from a combination of the approaching tropical convective system over Mato Grosso do Sul and the warm front over Paraná, ahead of a cold front slowly propagating north-eastwards. The winds backed to easterly above the tropopause.

The SF2 balloon was carrying the DESCARTES halocarbon grab sampler with which six samples were taken during the ascent. But unfortunately, a power failure at float prevented sampling during the slow descent. The measurements of halocarbons across the tropical tropopause indicate a tracer concentration gradient in proportion to lifetime. The fast response O_3SSS produced good data during ascent and descent, showing an ozonopause at about the secondary tropopause around 14 km, as well as resolved small-scale vertical structures. The μSDLA tuneable laser provided methane and water vapour data throughout the flight. In the water vapour profile a step of 10–12 ppm was observed above the lapse rate tropopause between 15.5 and 16 km and a minimum mixing ratio of 4 ppm at about 17 km. The μSDLA profile was also used as a reference for evaluating the measurements of the SAW, of a RS80 sonde at 15:15 LT and a RS 90 heated-Humicap on the backscatter sonde at 19:35 LT. The RS 80 was found to be significantly dry biased above 6–7 km, the SAW very consistent with the tuneable laser up to 12–13 km, and the RS 90 up to 16 km.

The μlidar performed successfully, making a profile of aerosol every 3 min. Unfor-

tunately, because of a failure in one of the battery packs, only the cross-polarized backscattering ratio is available. Cloud layers were seen at around 10–13 km during the entire flight with a downward slope of 3 km during the night, corroborated by a backscatter/ozone sonde at 19:35 LT showing two cloud layers between 10–12 km and 12.5–13.5 km.

On the same day the first flight of the Falcon took place to the NNE, making a range of observations next to the balloon flight area at the beginning and the end of its flight.

SF-1 flight

This flight was performed within an anticyclonic cloud-free area to the southwest of the SACZ, which had shifted towards north-east (Fig. 7). The balloon was launched at 17:24 LT on 16 February reaching an altitude of 20.5 km at sunset followed by a 6 h very slow descent to the SW, where it was cut down at 15.8 km close to the border of the State of Parana. Four-day trajectory data from RAMS show that at 350–140 hPa in the UT air flowed from the west, around the upper-level Bolivian high, with some descent from slightly higher potential temperature layers (Fig. 7, right), turning to the south at 90 hpa and then towards east above. The radiosonde shows a dynamical tropopause at about 13.5 km and a thermal tropopause of –76.1°C at 17.5 km (84.4 hPa, 399 K).

DESCARTES made 6 samplings during the ascent providing reliable data showing a layer of high halocarbon mixing ratio at 8.5–9.5 km, possibly resulting from a transport of urban polluted layer during preceding days. Unfortunately it failed again during the slow descent. LABS and the backscatter sonde did not report any cloud in the upper troposphere, but only at 3.5–4 km. Ozone data are available from both the SSS and the ECC sonde, showing an ozonopause at 14.6 km. The TDL made H_2O measurements during the ascent up to 250 hPa, but not above after a drift of the optical alignment. During this flight good data on both electric field and conductivity measurements were obtained. In particular, a complete profile of the electric conductivity due to positive charges was obtained over practically the whole altitude range with measurements every 8 min. A noticeable enhancement of conductivity is observed between 1 and

4 km, while a decrease is observed above at the altitude where the backscattersonde flown 2 h later showed the presence of thick cloud up to 14.5 km, which may change the nature of the atmospheric ions and modify the electrical parameters of the atmosphere. However, in absence of complementary measurements it is not possible to ascertain such an interpretation.

Cooperative observations are available from the third flight of the Falcon completing two ascent/descent cycles in an area close to the balloon flight track, showing a layer of enhanced CO at 8–10 km, indicative of urban pollution in coincidence with the halocarbon enhanced layer reported by Descartes.

SF-4 flight

This third slow descent flight was launched at 17:03 LT on 24 February when the SACZ was back over the central State of São Paulo (Fig. 8), creating a period of extensive instability with convective activity during day and night, albeit with reduced intensity. The balloon reached an altitude of 20.2 km shortly before sunset, followed by a 3-h slow descent down to 10.7 km, when it was cut down.

A large area of instability, with more or less randomly developing intense cells was first observed by IPMet's radars in the far north-west of the State of São Paulo, expanding eastwards while moving towards south-east as a whole. Significant intensification occurred from noon onwards, resulting in a massive multi-cellular complex heading towards Bauru during the late afternoon. Cloud tops during the early afternoon were mostly <14 km, but a few cells penetrated through the tropopause. However, the cloud tops subsided quickly to <10 km after sunset. At the time of the launch, the storm complex was about 120 km to the north-west, moving at 40 km/h^{-1} south-eastwards and reaching Bauru shortly after 20:00 LT. Figure 9 shows the radar echo tops detected half an hour after launch and towards the end of its float. The rain area situated 50–100 km south of Bauru (Fig. 9, right) was already in the decaying stage at the time of the launch and never affected the balloon track. Observations performed during this flight are thus representative of the TTL ahead of the approaching mesoscale system,

within a generally very convective environment. A radiosonde launched 20 min after the balloon indicates a secondary tropopause (lapse rate discontinuity) at about 14 km, a minimum temperature of –78.7°C at 15.9 km (112 hPa, 364 K), overlaid by a broad isothermal layer up to 18 km (77.5 hPa, 405 K).

The balloon was carrying six instruments: μDIRAC GC, μlidar, μSDLA, a SAW hygrometer, an O_3SSS and the AIRS electric field sensor. All performed satisfactorily. CFC 11 measurements by the μDIRAC show a constant mixing ratio (MR) up to 16 km, followed by a drop off beginning at 17 km. The SSS ozone sensor performed without problems, displaying, in agreement with the ozonesonde flown in parallel, an ozonopause at 14.2 km and significant structures above. The μSDLA shows a very dry layer between 8–11 km, followed by near saturation up to a drop off at 14.8 km above the secondary tropopause, and a mixing ratio of 4–5 ppmv in the TTL. The SAW hygrometer produced good data up to 14 km during ascent and below 13.5 km during descent, but showed insufficient sensitivity to make reliable measurements above these heights. During the descent, the μlidar made excellent measurements of a 1 km thick cloud layer at 13 km at the beginning, followed by the appearance of thin layers just above 14 km and at 13 km and more substantial clouds below 12 km. The backscatter sonde launched at 19:30 showed a thick opaque cloud up to 13.5 km at the beginning of the balloon flight. No lightning was detected by AIRS, but significant drops of the electric field probably related to differential charging of the top (negative) and the bottom (positive) of the cloud layers in the lower layers, and enhancement of the amplitude of electric field fluctuations near the tropopause where thin cirrus were reported by the backscatter sonde. There was no Falcon or Bandeirante aircraft flight on the day of the SF-4 flight.

SF-3 flight

The last slow descent flight was performed on 26 February. Launched at 17:00 LT, the balloon reached an altitude of 21.6 km shortly before sunset where it remained for about 1 h before descending slowly for 03:45 h down to 10 km. Very active thunder-

storms were developing in the morning over the State of Santa Catarina, moving fast northbound across the State of Parana (Figs. 10 and 11), but faded out by 22:30 LT about 150 km south-east of Bauru at the end of SF3. The temperature profiles show a lapse rate tropopause near 15 km, a cold point of –78°C at 80 hPa, topped by an almost isothermal TTL up to 18 km.

The SF-3 balloon was carrying a DESCARTES grab sampler, the μDIRAC GC, the TDLAS tuneable diode laser, the LABS backscatter diode laser, a SAW hygrometer and an O_3SSS sensor. DESCARTES performed successfully during the ascent and descent, providing measurements of tracers of a large range of lifetime spanning from 50 years to 3 months. The TDLAS made good measurements both during the ascent and descent. The most notable features of the profile are the low relative humidity (less than 20%) while ascending up to 15 km, and moist layers (60–80%) during the descent of the flight (10.5–11.5 km and 13–13.5 km), which are not evident on the ascent, as well as a minimum H_2O mixing ratio of 2.1 ppm at 17.7 km, around the level of the cold point tropopause. No clouds were observed by LABS during either the ascent or descent, but highly structured layers of depolarizing particles were seen during ascent between 16 and 18 km.

Other data available on 27 February are from a Falcon flight from 05:44–08:50 LT), an ozonesonde at 23:35 LT and a MIR SAOZ flight launched at 20:00 providing O_3, NO_2, H_2O profiles on the following morning.

Backscatter, ozonesondes and NILUCUBE

In total 10 BKS/ ozonesondes, 3 ozonesondes and 2 NILUCUBE were flown between 10 February and 6 March on 1400 m^3 Raven plastic balloons. Their date and maximum altitude reached by the balloon are listed in Table 3. The results of the BKS/ ozonesondes are displayed in Fig. 12. On average ozone shows an ozonopause around 13–14 km, very little varying mixing ratio linearly correlated with potential temperature in the lower stratosphere, but significant and frequent variations in the TTL. Cirrus clouds were absent at the beginning during the low convective period between 10 and 17

February but were frequent between 19–23 February at around 13-14 km when the temperature of the tropopause was cooler. A significant BKS signal was reported on one occasion at an altitude as high as 18–19 km on 20 February. A BKS/O_3 sonde was always flown in parallel to the SF flights.

The NILUCUBE was flown twice on RAVEN type balloons. The first flight was performed on 13 February under relatively clear sky conditions, but with some bright low-altitude cumulus clouds formed under limited convection conditions. The balloon was launched at 13:00 (UT) and climbed up to about 22 km, followed by a slow descent under a parachute. Solar zenith angles during the flight decreased from about 36° to 9°. The second flight was on 25 February under overcast conditions with high altitude cirrus. The launch was around local noon at 15:07 (UT). Solar zenith angles increased from about 12° to 30° during the flight. The instrument behaved well during both flights. For the flight on 13 February, the radiation increased by about 17% due to the change in the solar zenith angle between take-off and maximum altitude. On 25 February, the change in the solar zenith angle caused a maximum change of about 4% in the radiation during the ascent.

5.2 Long-duration balloons

The programme involved 8 constant-level superpressure balloons (SBP), and 3 MIRs.

The SBP were of two types: 10 m diameter floating at 55 hPa (19 km) and 8.50 m diameter at 75 hPa (18 km) that is at about the cold point tropopause level. All were carrying a GPS, a pressure and temperature sensors, as well as one or two passenger instruments: a turbulence sensor on the higher ones and a SAW and an O_3SSS sensor on those flying at the tropopause. The list of flights, their instrumentation, the date of launch and their duration are summarized in Table 4. The trajectories of the balloons are displayed in Fig. 13. Except for a transmitter failure on BP2 and a small leak on BP1, which depressurised and fell after 13 days, all other balloons remained at float level until the end of power of the lithium batteries designed for 1–2 months or their depressurisation at warm temperature at high latitude at the end of the summer

season. All GPS and meteorological sensors performed well, providing most useful scientific products (3-D trajectories, temperature and pressure fluctuations) for studying gravity and Rossby waves. However, the water vapour instrument did not detect the frost point temperature correctly, probably because of the limited mass of H_2O deposition due to the absence of ventilation, and the ozone sensors stopped transmitting their information to the main gondola after 14 and 3 days, respectively.

The instrumentation carried by the MIRs, their date of launch and duration in flight are summarized in Table 5. Their trajectories are shown in Fig. 14. Among the four attempts, one failed at launch, which was replaced by a spare balloon. The 3 MIR remained in flight for 7, 39 and 9 days, respectively. The relatively short flight of two of them (the first was recovered in Australia) was due to a fast descent over high-level clouds in the evening. These anomalous events have been identified to be due to a too small size of aperture at the bottom of the MIRs resulting in a reduction of volume when the balloon is descending after sunset. MIR-1 provided only limited data after the partial failure of the SAOZ detector at low temperature. But the two others were particularly successful. The ENEA micro-lidar flown for the first time on MIR-2, got very encouraging cloud data, although part of the measurements were found noisy because of electrical interference with the Inmarsat transmitter. The SAOZ instrument on board MIR-3 provided the longest ever series of profiles (78) of O_3, NO_2 and cloud extinction in the tropical UTLS, and for the first time H_2O. For comparison purpose, dedicated ozonesondes ascents have been performed during the overpass of the balloon over the SHADOZ stations of Samoa, Fiji and Reunion Island, as well as at Bauru at the launch Unfortunately, high-altitude clouds, associated with hurricane Gafilo in the Indian Ocean, prevented collocated ozone lidar observations at Reunion Island to be carried out as in 2001, for checking the altitude registration of the retrievals. Finally, all meteorological sensors, as well as the global IR radiometer and the lightning optical detectors performed well on all flights.

6 Results

The rich observational data set collected during the pre-HIBISCUS and HIBISCUS campaigns has been used for a variety of investigations, such as verification of NWP models representation of the tropical UTLS, vertical and horizontal troposphere-stratosphere exchange, waves, water vapour, clouds and microphysics, photochemistry and finally satellite validation as proposed in the objectives. Their results are briefly summarized below. More details will be found in the papers cited.

6.1 Evaluation of meteorological models analyses and re-analyses

Among the objectives of HIBISCUS were the evaluation of temperature and wind in the NWP ECMWF operational model and other ECMWF:ERA40 and NCEP/NCAR reanalyses in the tropics. This has been achieved by comparing the above models to the data of a number of long-duration balloon flights: the Hibiscus flights for operational analysis, the data of an EOLE experiment at 200 hPa in 1971–1972, and those of 30 MIR and three 10 m-diameter SPB flown since 1988.

6.1.1 ECMWF and NECP operational analysis

Actual temperature, wind and trajectories of the 8 SPB and the 3 MIR have been compared to ECMWF T511 operational products (Knudsen et al., same issue). Compared to the balloon measurements just above the tropical tropopause, the ECMWF operational temperatures show a systematic cold bias of 0.9 K and the easterly zonal winds are too strong by 0.7 m/s. This bias in the zonal wind adds to the ECMWF trajectory errors, but they still are relatively small with, e.g. an error of about 700 km after 5 days. The NCEP/NCAR reanalysis trajectory errors are substantially larger (1300 km after 5 days). In the southern mid-latitudes the cold bias is the same, but the zonal wind bias is almost zero. The trajectories are generally more accurate than in the tropics, but for one balloon many of the calculated trajectories end up on the wrong side of the tropical

barrier and this leads to large trajectory errors.

6.1.2 ECMWF ERA40 and NCEP/NCAR NN50 at 200 hPa in 1971–1972

Reanalysis evaluations are based on data that could be recovered from long-duration balloon flights carried out in the past. Indeed, long-duration balloons have been deployed experimentally since the mid-60's at both NCAR and CNES. Small super-pressure balloons of 3.70 m diameter were developed at CNES, floating at 200 hPa for the EOLE experiment during which 480 platforms were deployed in the Southern hemisphere in 1971–1972 and tracked by a dedicated satellite, the ancestor of ARGOS.

The EOLE dataset has been used to assess the accuracy of modern reanalyses. 80 000 reliable temperature and wind data, covering one year in 1971–1972, have been recovered, providing information on atmospheric regions scarcely sampled during the pre-satellite era, i.e. the Antarctic and the southern hemisphere oceans (Hertzog et al., 2006). When compared to the EOLE dataset, the ECMWF ERA40 re-analyses shows limited temperature bias at 200 hPa in sub-polar regions, whilst the NCAR NN50 is a few degrees colder. However, both re-analysis data sets are found warmer by about 1 K in the subtropics. The biases on the wind field are found to be very small, if not insignificant. The standard deviation of the difference between models and balloon data displays a decrease over continents compared to oceanic areas, stressing the heterogeneity of atmospheric observation systems during the pre-satellite era, and is larger in the storm tracks than elsewhere, which emphasizes the difficulty of atmospheric models to capture the synoptic systems in the poorly sampled southern hemisphere, before the event of satellite observations. However, both reanalyses do not perform similarly in this respect. The NCEP/NCAR standard deviations are significantly smaller than those of ERA40.

6.1.3 ERA40 in the tropical stratosphere since 1988

In another effort, the data of past CNES technical and scientific balloon flights, have been searched for (Christensen et al., 2007[3]). No data prior to 1988 could be recovered. The data available in the tropics are those of 30 MIR and 3 SPB of 10 m diameter flown from Pretoria in 1988–1992, Latacunga in Ecuador in 1994–1998, and Bauru in Brazil in 2000–2001. After being carefully checked, largely by comparing measurements performed by independent payloads on the same balloon, about 40 000 reliable temperature and 12000 wind measurements of 18 MIR and 3 SPB, flown between 1988-2001, were retrieved.

When compared to the balloon data, the ERA-40 (T159 3-D variational assimilation) temperatures in the tropical stratosphere show displays a bias varying progressively from +1.16 K in 1988–1989, to +0.26 K in 1994–1996 and –0.46 K after 1998 (Christensen et al., 2007[3]). The ERA-40 zonal wind in the lower stratosphere appears slightly overestimated by 0.7–1.0 m/s on average in both the tropics and equatorial region, while the meridional wind is unbiased (0.01±3.2 m/s). This relatively large bias compared to previous studies in the Arctic (Knudsen et al., 2002), may be due to the reduced number of radiosondes and the breakdown of geostrophy in the tropics, which makes it difficult to transform satellite observations of temperature to winds. Despite this, we found the tropical trajectory errors to be surprisingly small.

6.2 Convection and vertical transport

In this area, the objectives were to study the impact of convective transport on the TTL and the lower stratosphere, based on radiosonde temperature profiles and balloon measurements of vertical profiles of ozone and of a range of tracers with different

[3]Christensen, T., Knudsen, B.-M., Pommereau, J.-P., Letrenne, G., Hertzog, A., and Vial, F.: Validation of ECMWH ERA-40 tropical stratosphere temperatures and winds with long duration balloon data, Atmos. Chem. Phys. Discuss., submitted, 2007.

lifetimes. These measurements were to be interpreted using models at meso- and global scale. The main results of this study are summarised in the following sections.

6.2.1 Afternoon cooling of the TTL over land convection

The amplitude and the altitude of the cooling of the TTL by overshooting of adiabatically cooled air over land convective systems has been studied from the four daily sonde ascents carried out between 30 January and 22 February and the 13 ozonesondes between 10 February and 6 March (Pommereau and Held, 2007[4]). Compared to non-convective periods, the temperature is found cooler (8 K cooling at 16–17 km) in the TTL up to altitudes of 19 km, 3 km above the lapse rate tropopause, during the highly convective period at the beginning of February. Similarly, a drop of ozone mixing ratios as large as 60 ppb could be observed between 12–17 km during the medium convective period between 17 and 24 February. But more importantly, a systematic diurnal variation of temperature could be observed up to 19 km, of 4 K amplitude at 16–17 km in early February at 16:00 LT compared to 10:00 LT, and still of 2 K amplitude during the second half of the month when the convection was less intense. The large amplitude of the cooling in the afternoon, coinciding with the phase of maximum development of diurnal convection (e.g., Liu and Zipser, 2005), provides evidence of strong overshooting over land convective systems as suggested by Danielsen (1982). Moreover, the potential temperature level up to which the cooling could be observed, 440 K during the highest convective period, indicates that overshoots could penetrate relatively deeply into the lower stratosphere. The suggestion is that, in contrast to oceanic areas where little overshooting above the tropopause is observed, the fast developing land convection in the afternoon in the tropics, little captured by the models, could be a major contributor to troposphere-stratosphere exchange at global scale.

[4]Pommereau, J. P. and Held, G.: Evidence of strong afternoon overshooting convection in the tropical stratosphere over land, in preparation, 2007.

6.2.2 Vertical transport in the tropical UTLS from tracers of different lifetime

A wide range of tracers was measured in both the 2003 and 2004 campaigns on board ZL and SF balloons. Halocarbon (and N_2O) measurements were made by the DIRAC in situ gas chromatograph (GC) and two DESCARTES grab samplers (Harris et al., in preparation). A range of halocarbon tracer lifetimes was measured from 85 years (CFC-113) to 3–6 months (chloroform). The picture painted by the data is of a TTL rich in spatial structure. It is clear that simple vertical (1-D) transport models, used hitherto, cannot explain the observations. The long-lived halocarbons measured in the troposphere were generally well mixed (showing little vertical gradient). There was some suggestion of boundary layer enhancement. On some flights mixing ratios above-background levels could be observed in long-lived tracers just below the TTL layer, which could indicate uplift of boundary layer air (e.g., CFC-113 on SF1 and SF3). The long-lived tracers again showed no vertical gradient across the TTL between 350 and 400 K. Only above 400 K was there a noticeable drop-off in the long-lived tracer-mixing ratio, indicating stratospheric aged air. The long-lived tracers are also anti-correlated with the co-located ozone measurements in this region.

In the case of the shorter-lived halocarbon tracers below and inside the TTL region, much more variability was found in the vertical profiles. While the long-lived tracer data shows little gradient or variability in the 350 to 400 K region, the shorter-lived tracers show considerable variation. In the case of chloroform (~6 months lifetime), there is a decrease in mixing ratio of around 3 ppt between 350 and 400 K (amounting to some 50% of the tropospheric value). Chloroform was also measured at higher vertical resolution by DIRAC on the SF4 flight (24 February). In the case of dibromomethane (3 to 4 month lifetime), the tracer distribution is more difficult to describe, since there is a slight drop-off between 350 and 400 K, but there is evidence of a maximum in the 360 to 380 K region. Unfortunately, dibromomethane was only measured by the DESCARTES grab samplers and so the vertical resolution is low.

A first attempt to explain the tracer vertical structure using the simple 1-D model

introduced by Folkins et al. (1999) was unsuccessful. It was not possible to reproduce all the profiles with a single vertical velocity. It is clear that this model (while having been extremely influential) must now be considered too simple. The overall structure of the TTL is complex and three-dimensional.

6.2.3 Modelling of Troposphere-Stratosphere transport at global scale

To complement the local modelling in support of the balloon flights, modelling studies have also been performed to investigate the global structure of the TTL and transport using both high-resolution trajectories and a lower-resolution CTM (Levine et al., 2007). In each case the regions of preferential transport from the lower troposphere into the TTL and from the TTL into the stratosphere were examined. Results show, that transport into the TTL occurs primarily over the maritime continent, followed by extensive horizontal transport within the TTL. Regional differences in transport from the TTL to the stratosphere are much smaller than the corresponding differences for transport into the TTL from below. Most of the transport into the stratosphere takes place into the extratropical lower stratosphere (below 400 K). Reassuringly, the trajectories and the p-TOMCAT CTM tracers give the same basic picture. However, the open question is to know to what extent the stratospheric penetration of land convective overshooting in the afternoon is not included in the models.

6.2.4 Troposphere-Stratosphere exchange from satellite measurements

The possible contribution at the global scale of convective lifting of tropospheric air in the TTL was also investigated from satellite observations of tropospheric species at 17 km, below, at, or immediately above the tropopause (Ricaud et al., 2007[5]). The

[5]Ricaud, P., Barret, B., Attié J.L., Le Flochmoën, E., Motte, E., Teyssèdre, H., Peuch, V.-H., and Pommereau, J.-P.: Impact of convection, biomass burning and wetland into the Tropical Tropopause Layer over the March-May 2002–2004 period, Atmos. Chem. Phys. Discuss., submitted, 2007.

average 2002–2004 N_2O concentration at 17 km reported by ODIN-SMR, as well as CH_4 from HALOE and CO from MOPITT at 150 hPa during the March-April-May period studied, displays regional differences with a prominent maximum over equatorial Africa and to a lesser degree over central America and south-east Asia continental and island areas but not above the Maritime continent. In contrast with the previous modelling, but in agreement with the observed geographic distribution of frequency of overshooting clouds by the TRMM precipitation radar (Liu and Zipser, 2005), land convective overshooting appears to be a privileged mechanism of transport in the TTL

6.3 Meridional exchange between the mid-latitude lower stratosphere and the TTL

The objective in this field was to study the transport processes through the tropical barrier in the lower stratosphere. Three different studies have been conducted from the HIBISCUS data relative to the tropical barrier and the exchange between the mid-latitude overworld and the TTL: from SPBs trajectories; from ozone profiles of the SAOZ-MIR and ozonesondes; and from vertical diffusivity derived from high-resolution balloon and aircraft ozone and tracer measurements.

6.3.1 Meridional exchange from SPBs trajectories

The trajectories of the 8 SPBs displayed in Fig. 13, have been analysed and their dispersions studied. The first four had very zonal trajectories staying at latitudes close to 20° S. In contrast, the other four drifted southward after leaving South America and were finally trapped in the mid-latitude circulation. Those trajectories therefore show an obvious example of exchange through the stratospheric subtropical barrier. A preliminary study that uses the ECMWF analyses indicates that the two kinds of trajectories seem to be linked with the strength of 2 anticyclones, one located to the west of South America, the other eastward of New Zealand, for explaining the difference of the two types of trajectories. At the beginning of the campaign, the latter anticyclone was strong enough to prevent tropical air masses (and SPBs) to drift southward cycling around the

one above South America. During the first days of March, when the last SPBs were launched, it weakened and tropical air masses were pushed southward. Further work is ongoing to precisely characterize the dispersion regime in the lower stratosphere that prevailed during the campaign.

6.3.2 Horizontal exchange between the mid-latitude overworld and the TTL from ozone profiles

The relative contribution of quasi-horizontal (adiabatic) and vertical (convective) transport to the variation of ozone concentration in the tropical UTLS has been quantified from the SAOZ-MIR measurements in 2001, 2003 and 2004, as well as from the 13 ozonesondes launched from Bauru in 2004, by a multi-linear regression technique (Borchi et al., same issue). The statistical analysis makes use of potential vorticity (PV) as proxy of horizontal transport or displacement, and the difference in altitude between the 340 and 370 K isentropic surfaces as an index of convection. The first is provided by the MIMOSA contour advection model (Hauchecorne et al., 2002), run every 5K between 300K and 700 K and initialized by the 6-hourly ECMWF analyses, whilst the second is directly derived from ECMWF. Overall, the analysis of ozone profiles at zonal and local scale in the tropics displays a maximum variability in the TTL between 12–19 km, mainly due to horizontal exchange with the mid-latitude stratosphere and to a more limited extent to convective vertical transport. Local photochemical production appears to contribute for a small amount to the observed variability, no more than few percent at most.

6.3.3 Vertical diffusivity and mixing in the TTL

In strongly stratified shear flows like the stratosphere, vertical (cross-isentropic) diffusion is one of the causes of horizontal mixing. It is generally assumed that overall small-scale mixing processes can be represented by only one coefficient, viz., the turbulent diffusivity D, which varies in space and time. However, estimates in the literature

range from 0.001 to 5 m^2s^{-1} in the lower stratosphere, the latter corresponding to radar estimates.

In this study, in order to obtain parametrization-independent estimates of D, tracer mixing ratios are reconstructed along the flight track of aircraft measurements. The method uses ensembles of Lagrangian backward trajectories starting at each measurement point. Vertical turbulent diffusion is introduced as a random independent perturbation in each member of the ensemble. The trajectories are calculated using ECMWF winds, and the reconstruction is done by interpolating mixing ratios provided by the REPROBUS-CTM at the endpoints of trajectories. Then, measured and reconstructed profiles on the same flight track are compared. The magnitude of fluctuations in the reconstruction profile is related to the value of the vertical turbulent diffusivity coefficient D. This allows an estimation of the coefficient D by tuning the fluctuation to best fit the observed tracer profiles. From previous studies in the lower stratosphere, at 60 hPa, D is found to be, on average, of the order of 0.01 m^2s^{-1} in the polar region and 0.1 m^2s^{-1}in mid latitudes, with a sharp transition in the polar vortex edge (Legras et al., 2005).

In the lower stratosphere, vertical diffusivity in the Bauru region – estimated from HIBISCUS high-resolution airborne measurements – is found to be in the order of 0.5–1 m^2s^{-1} (Pisso and Legras, 2007[6]). Sharp changes in the value of D are often found in the presence of different layers of different origins. This is particularly true in the case of subtropical intrusions in the tropics, where air masses of different origin and dynamical characteristics meet. Transport barrier effects may generate boundaries between different diffusivity regions. Ensemble calculation of Lyapunov exponents is introduced, following back-trajectories together with tracer reconstruction, unveiling the stretching history of parcels. This allows relating diffusion and strain, by mapping the location of dynamical structures.

[6]Pisso, I. and Legras, B.: Turbulent vertical diffusivity in the subtropical atmosphere, Atmos. Chem. Phys. Discuss., in preparation, 2007.

6.3.4 Lagrangian reconstructions of tracers

Another question, which has been studied, is the impact of space and time resolution of wind fields on the quality of Lagrangian reconstructions of tracers. Indeed, trajectory calculations make use of winds interpolated from Eulerian fields. It has been shown, that Lagrangian reconstructions exhibit strong sensitivity to time resolution of ECMWF analysed winds (more than to spatial resolution). This result suggests that using the standard 6-hourly archive might lead to serious overestimates of vertical transport, due to both under-sampling of fluctuations and the presence of spurious gravity waves excited by assimilation. Reconstructions with various combinations of analysis and short-term forecasts were performed. ECMWF wind fields were archived every hour to further test the Lagrangian reconstructions sensitivity to time resolution (Pisso and Legras, 2007[6]).

6.4 Wave sources and propagation

The Rumba payload carried by SPB balloons provides high-accuracy measurements of temperature and wind sampled every 15 min and pressure every minute. Altogether, these data are used to characterize the gravity-wave activity during the flights (Hertzog et al., in preparation). Figure 15 for instance shows the horizontal kinetic energy spectra for two of the SPB flights (flight 4 and 6). The energy is represented with respect to the intrinsic frequency, i.e., the frequency that is measured in the mean flow. Gravity waves have intrinsic frequencies larger than the inertial frequency. While Flight 4 stays at low latitudes, Flight 6 was pushed to the mid-latitude, and, consequently, the mean inertial frequencies during those two flights slightly differ. The picture clearly exhibits the –2 slope of gravity-wave energy, which is an observational evidence that only SPBs can obtain. The picture also shows the increase of kinetic energy close to the inertial frequency on both flights, which is the signature of the ubiquitous presence of inertia-gravity waves. Finally, the low-frequency part of the spectra is likely associated with Rossby waves, which are more visible on the mid-latitude flight. Further studies are

ongoing to investigate the variation of wave activity during the flights, identify the wave sources, and to quantify the energy and momentum transported by the waves to the upper atmosphere.

6.5 Water vapour

A number of water vapour measurements in the TTL and the lower stratosphere were made during HIBISCUS by deploying several techniques: locally above Bauru by Vaisala RS80 and RS90, by two tunable diode laser systems and the SAW sensors, and at global scale remotely by SAOZ on the MIR and GOMOS. Their results have been first compared to understand which and where each of them can provide reliable data, and then interpreted by means of statistical and trajectory methods, microphysical model including growth and precipitation run in trajectory and LES dynamical frameworks.

6.5.1 Quality of water vapour measurements in the TTL

The measurement of low water vapour mixing ratios in the cold TTL and lower stratosphere is still challenging. As indicated in Sect. 5, several instruments experienced failures for a number of reasons. The best measurements were found to be those of the diode lasers (micro SDLA and TDLAS) during the night-time slow descent, free of outgassing contamination, at least when the descent speed is high enough, although the accuracy of the TDLAS (10%) is currently lower than that of micro-SDLA, which is estimated to be 5%. Compared to these, the profiles obtained simultaneously by the SAW hygrometer and the Vaisala radiosondes exhibit a significant degree of uncertainty above 10–11 km altitude. The measurements made by pairs of RS80 and RS90 Vaisala radiosondes launched on board weather balloons agree extremely well below approximately 11 km, but tend to differ vastly above this altitude, with the RS80 being significantly dry biased compared to the RS90. The latter showed excellent agreement with the micro-SDLA in the UT up to the moist secondary tropopause at about 15 km.

The SAW hygrometer also showed generally good agreement with SDLA and TDLAS for frost points in the range of +20/–80°C, although there were regions in the middle troposphere of significant discrepancies (>20°C), generally in regions of low RH and high structure. Overall, whilst good information could be obtained in the troposphere with the RS80 (up to 10–11 km), the RS-90 and the SAW (up to 14–15 km), reliable data on the water vapour in the TTL could only be obtained with micro-SDLA and TDLAS.

6.5.2 Water vapour observations in the upper troposphere and the TTL over Brazil

The H_2O mixing ratios reported by the micro SDLA during its two flights show a moist troposphere with 1–2 km thick dry layers at about 7 km in SF2 and 9 km in SF4, and large supersaturations at the secondary tropopause up to 16 km on the first and 15 km on the second flight (Durry et al., same issue). Above these levels, the water vapour mixing ratio ranges between 3.5 and 5 ppmv, which is comparable to that observed at mid-latitude at the same potential temperature levels in late spring for the lower value and autumn for the highest. No significant dehydration was observed at the relatively warm sub-saturated cold point at –78°C, but alternative dry (3.5 ppm) and moister (5 ppm) layers, separated by sharp gradients, were found. Correlations with CH_4, also measured by SDLA, ozone from SSS and ECC sensors, temperature and PV from the MIMOSA model, allow us to identify unambiguously the origin of each layer. The CH_4 poor and ozone rich dry layers in the UT can be attributed to descent of stratospheric air. At the other extreme, the 180% supersaturated, cold, CH_4 rich and O_3 poor layers near the tropopause imply the convective lifting of tropospheric air parcels. More surprising is the superposition of dry and moist layers in the TTL and the lower stratosphere up to 400 K, highly correlated with CH_4 and PV, and anticorrelated with ozone and temperature.

The overall measurements suggest a complex picture with indications of both convective uplift of moist air from the lower/middle troposphere to the TTL region (5 ppmv up to 18 km, 400 K), and the presence of dry layers linked to stratospheric intrusions. In the case of SF4, the overshoot penetrates the stratosphere up to 400 K (Durry et al., same issue).

The possible location and time of the convective event, responsible for the supersaturated layers and the cirrus clouds reported on the same flights by the micro-lidar, has been further explored by backward 3-D trajectories calculated from outputs of the BRAMS mesoscale model using a 3-D back trajectory code developed by Freitas et al. (2000).

6.5.3 Water vapour in the TTL at global scale

The zonal variation of water vapour has been derived from the measurements of the SAOZ version extended to 1 μm, which was flown on the MIR for 39 days (Pommereau et al., 2006; Pommereau et al., 2007[4]). Although the first profile over Brazil at the beginning of the flight is consistent with that reported by the micro-SDLA and the precision of the measurements (0.2 ppm) is relatively high, their accuracy (2 ppm) is limited because of the broad spectral resolution measurements in a spectral band where strong narrow H_2O lines are saturated. Overall, 78 profiles were collected along the MIR flight from 25 km down to 6 km or cloud top.

The main feature shown by these measurements is the presence of a minimum H_2O mixing ratio (hygropause) of 3.5–5 ppm, on average above the cold point tropopause around 18 km, that is 3–4 km above the secondary tropopause and the ozonopause. No clear dehydrated layer could be observed at the latitude of the balloon flight between 10–20° S, where the cold point temperature remains relatively warm. The minimum H_2O value at the hygropause shows a zonal modulation. In contrast to expectation, maxima (5 ppm) are observed over convectively active convergence zones over Africa, South America and the West Pacific and minima (3.5 ppm) above subsident oceanic areas. The picture is consistent with the μSDLA observations over Brazil, as well as those of the broad vertical resolution microwave measurements of MLS-UARS, showing a maximum mixing ratio above land convective regions at the tropics in the Southern Hemisphere summer of 1992–1993, but it is in contrast with ECMWF, in which the cold trap mechanism stops the uplift of water vapour as soon as saturation is reached.

6.5.4 BRAMS mesoscale modelling

Following the study of the impact of deep convection on the composition of the upper troposphere in an extreme storm case from BRAMS simulations (Marécal et al., 2006; Rivière et al., 2006), mesoscale modelling studies have been continued. The ability of the model to simulate the vertical variations of water vapour observed by the micro-SDLA compared to ECMWF global analysis has been investigated (Marécal et al., same issue). The BRAMS mesoscale model (improved version of the RAMS developed at CPTEC, Centre for Weather Prediction and Climate Studies, Brazil) performs significantly better than ECMWF analysis for water vapour in the upper troposphere but slightly worse for temperature. The improvement provided by the mesoscale model for water vapour comes mainly from (i) the enhanced vertical resolution in the UTLS (250 m for BRAMS and ∼1 km for the ECMWF model) and (ii) the more detailed microphysical parameterization allowing ice supersaturations as in the observations. The ECMWF vertical resolution is too coarse to capture the observed fine scale (∼1 km) variations of water vapour in the UTLS. In near-saturated or supersaturated layers, the mesoscale model water vapour is close to observations, but only if the model temperature is realistic. For temperature, the ECMWF analysis gives good results thanks to data assimilation. Analysis of the results showed that in undersaturated layers the water vapour profile depends mainly on the dynamics. In saturated/supersaturated layers, microphysical processes have to be taken into account, in addition to the dynamical processes, to understand the water vapour profile.

6.5.5 LES cloud resolving modelling

The UK Met Office Cloud Resolving Model (Shutts and Gray, 1994; Swann, 1996, 1998) version 2.3 has been used to simulate overshooting deep convective events based on the 24 February case study day (Grosvenor et al., 2007[7]). The control run

[7]Grosvenor, D., Choularton, T., Coe, H., and Held, G.: Cloud Resolving Model simulations of dehydration by deep convection of the TTL and lower stratosphere, Atmos. Chem. Phys. Discuss., in preparation, 2007.

produced a vigorous cloud that represented the upper end of the spectrum of convective strength occurring in reality. The overshooting cloud produced a ∼0.75 km thick layer of dehydrated air in the TTL above the convective anvil through vapour deposition and subsequent ice fall out. Here the total water content of the air was reduced by 1 ppmv or more over a distance of ∼200 km thus representing significant dehydration, which could have a global impact given the frequency of very deep convective events observed in the Bauru area by the IPMET radar. However, moistening due to remaining ice occurred below this height such that the overall effect on the TTL would be to moisten if its base is defined as the level of net zero radiative heating (∼15 km) given in Gettelman (2004) and if the remaining ice did not fall out before evaporating. Accurate determination of this height is likely to be vital in order to gauge the effect of convection on stratospheric water content since above the height of 15.5 km (within the uncertainty of the zero radiative height given in Gettelman, 2004) only dehydration with no moistening was observed.

The vast majority of the ice reaching the TTL was formed much lower down in the cloud and then transported upwards, which indicates the importance of the microphysical processes occurring throughout the cloud in determining the fall speeds of ice and hence the amount of dehydration. This has been demonstrated by examining the sensitivity to the number density of droplets in the cloud. When this number was increased from 240 kg^{-1} to 960 kg^{-1} the mode mass of ice particles reaching the TTL was found to be significantly smaller. Therefore, the ice particles had lower fall speeds and as a consequence there was significant ice present below 16km with approximately the same amount of dehydrated air as before above this height. There was approximately no net effect over the TTL as a whole when using 15.5 km as the TTL base. With a lower TTL base net moistening of a magnitude significantly greater than in the control run would be likely to occur. This points towards a possible anthropogenic aerosol impact on the effects of overshooting convection on the TTL water vapour budget.

6.6 Clouds and aerosol microphysics

Several cloud measuring instruments have been flown during HIBISCUS: the micro-lidar, and the backscatter sondes on short-duration balloons, in conjunction with the Brazilian TroCCiBras Doppler radars and lidar, as well as the SAOZ solar occultation spectrometer and the micro-lidar on MIRs for extending the observations to the global scale. Altogether, these instruments have provided unique observational data for the better understanding of the formation of cirrus clouds in the TTL region. Among the results is the frequent detection of anvils up to 14 km and ultra-thin cirrus at the lapse rate tropopause around 15 km above convective systems, but not higher. A new feature, observed twice above very active convection, is the sporadic presence of small particles up to 19 km in significantly sub-saturated regions, which could be indicative of strong uplift over cumulonimbus cloud turrets. This feature is interpreted as a signature of convective moistening of the lower stratosphere (Nielsen et al., same issue).

For a better understanding of the mechanisms involved, these observations have been simulated by two microphysical models: the Microphysical Cirrus (MPC) model of DMI, utilizing background meteorological fields from the BRAMS model and from ECMWF, and the UK Met Office LEM Cloud Resolving Model. The event has been simulated by the LEM, suggesting that the formation of high-altitude cirrus could result from gravity waves caused by pulses of deep convection or by turbulent mixing of the outflow air as it is pushed outwards from the turret (Grosvenor et al., 2007[7]). Further improvements are anticipated from the work in progress on combining the two models (the microphysics of MPC and the dynamics of the LEM), to better reproduce the observations, which would enable large-scale cirrus formation to be studied over long timescales.

This work may also provide some explanation for the observed evidence of some very high-altitude particles seen by the DMI and ISAC backscatter-sondes at altitudes of up to 20 km. Ice formation by gravity wave action was observed at such altitudes in the LEM model and it is possible that its evolution over longer timescales could produce

the stable structure observed.

Another subject under investigation is the reliability of the cloud top altitude reported by the radar. Radar echoes simulated by LEM compared fairly well, but with reflectivity values that were generally slightly too high. A better understanding of this issue has been obtained from the comparison between radar and micro-lidar top height measurements (Di Donfranceso et al., 2005a, b).

An analysis of in-situ observations of cirrus shows high mesoscale variability in height, thickness and optical properties, when layered cirrus are formed in the outflow of complex convective systems. Mesoscale simulations indicate, that observed differences can be linked to the different residence time of convective-processed air in the upper troposphere, which in turn gives evidence of different cirrus formation mechanisms (Fierli et al., 2007[8]).

6.7 Photochemistry

The objective here was the study of fast NO_x and bromine chemistry in the tropical UT/LS by comparing photochemical and radiative model simulations to observational data from the balloon flights. Significant progress has been achieved in four different areas: bromine chemistry, NO_x production by lightning in the UT, NO_x fast photochemical change at twilight and impact on remote sensing from space, and photolysis rates.

6.7.1 Bromine chemistry

Bromine chemistry was investigated from BrO measurements of the SAOZ UV enhanced version, flown twice in the late afternoon on 31 January and 5 February, together with the three main parameters controlling its photochemistry: O_3, NO_2 and temperature (Goutail et al., in preparation). The two flights took place in very different

[8]Fierli, F., Di Donfrancesco, G., Cairo, F., Zampieri, M., Orlandi, E.: Cirus clouds in convective outflow durin the Hibicus campaign, Atmos. Chem. Phys. Discuss., submitted, 2007.

conditions. The first occurred during a period of low convective activity, while the second was performed in the vicinity of some deep convective cells. The ozone-mixing ratio was almost identical in both flights, but that of NO_2 and BrO were significantly different. In both cases, BrO showed a steep increase in the TTL at about 16 km on 31 January and 17–18 km on 5 February, following the oxidation of inorganic bromine. There was no indication of significant inorganic bromine concentration below in the upper troposphere. Large changes could also be seen in BrO and NO_2 in the stratosphere. They are anti-correlated, with BrO being maximum when NO_2 is minimum. The likely reason for the large changes in NO_2 concentration is the horizontal advection of NO_x poor/rich, equatorial/mid-latitude air, as indicated by Potential Vorticity (PV) changes displayed by the MIMOSA model. The NO_2-BrO anti-correlation could be partly due to the shift in the daytime photochemical equilibrium between BrO and its reservoir $BrONO_2$, because of the large NO_2 changes. But since, according to model simulations, its amplitude would not be enough, it would require also an advection of Bry rich air suggesting higher amount of Bry in the lower stratosphere at equatorial latitude than in the mid-latitude summer.

6.7.2 NO_x photochemistry

The NO_x photochemistry in the tropics was explored from the SAOZ-MIR NO_2 profiles at sunset and sunrise (Pommereau et al., 2007[9]). After correcting the measurements for the fast photochemical change during the twilight periods, particularly significant in the tropics because of the low temperature and limited amount of ozone, the amplitude of the diurnal variation, i.e., NO_2 Sunset / Sunrise ratio, fully agrees with that simulated by the MIPLASMO 1-D model (Rivière et al., 2003) at all levels. At least at the time scale of one day, the NO_x photochemistry in the tropical UTLS appears well

[9]Pommereau, J.-P., Nunes-Pinharanda, M., and Borchi, F.: Impact of horizontal transport on ozone in the tropical upper troposphere and lower stratosphere from SAOZ long duration balloon measurements, in preparation, 2007.

understood. An important implication of the study is that the correction for fast photochemical change at twilight amplifies with the altitude of the observing platform, being the largest for solar occultation from orbit when half of the optical path is on the night side. This largely explains, for example, the over-estimation of the NO_2 diurnal variation in the tropical lower stratosphere reported by SAGE 2. Another conclusion is that the full NO_x chemistry must be taken into account in the CTM models for comparisons with solar occultation measurements. The assumption of photochemical equilibrium between NO and NO_2 used, for example, in the REPROBUS CTM simulations (Lefèvre et al., 1994), for reducing the cost of the calculations, is not valid in the tropics in the cold and ozone poor TTL. When full chemistry is introduced in the model, REPROBUS fully agrees with the observations, as well as MIPLASMO.

6.7.3 NO_x production by lightning

The reasons for the variability of NO_2 was also explored by the multi-linear regression technique already used for investigating the impact of horizontal and vertical transport on ozone concentration (Pommereau et al., 2007[9]). In contrast to ozone, it was found that quasi-isentropic exchange with the mid-latitude has a strong impact on NO_2 concentration in the lower stratosphere, because of the significant latitudinal gradient of NOy between mid-latitude and the tropics. But this does not apply in the TTL and the upper troposphere, where the largest cause of NO_2 concentration variability was found to be NO_x production by lightning. Indeed, large concentrations of up to 500 ppt could be observed at about 12–14 km in the UT over South America and Africa and in contrast, very little, 100 ppt or less, over the South Pacific Convergence Zone and Australia, although deep convection is also frequent there. The picture was almost identical in 2001 and 2004. Evidence of this is provided by the high correlation between NO_2 and the frequency of flashes reported by the NASA Lightning Imaging Sensor in orbit, showing strong electric activity over land areas, but very little over oceans. At least qualitatively, this finding fully agrees with MOZART and LMDz-INCA global-scale simulations.

6.7.4 Photolysis rates

Because of the high sun, the reduced ozone column, as well as the presence of reflective clouds at high altitude, the photolysis rates of UV sensitive chemical species significantly increase in the tropics. The objective here was to derive the photolysis rates of a number of species from the NILUCUBE UV radiation balloon measurements, flown under clear conditions, but also some low-altitude cumulus on 13 February and overcast conditions by high-altitude cirrus on 23 February. As an example, the O^1D photolysis rates derived for the two flights were shown to be clearly affected by the thin cloud covers at around 2 and 12 kilometres respectively, resulting in an enhancement of about 27% at 23 km altitude. The photolysis rates calculations were extended in wavelength with more cross sections and quantum yields, allowing the calculation of numerous photolysis rates of interest for photochemical simulations. Since the cube does not provide full coverage of the spectra needed for the calculation of all rates, a radiative transfer model (Mayer et al., 2005) is used in combination with the measurements, where the same input for the simulated NILUCUBE data are used at all wavelengths of interest, under the assumption that, if the model is able to reproduce measurements at one wavelength, it is able to reproduce at other wavelengths too. Rates from 21 of the most important species have been made available for the two flights.

6.8 Satellite validation

Remote observations of atmospheric species available from space instruments employing a range of techniques are available. However, significant discrepancies are often observed between them, particularly in the tropical UT/LS, where the precision of the retrievals degrades rapidly at decreasing altitude, because of the presence of high-altitude clouds, increased attenuation, low temperature, interference with water vapour, etc. A number of space instruments were operating during the HIBISCUS period: the long-standing NASA SAGE II and HALOE, the newer NASA-SAGE III, the Sweden-

Finland-Canada-France ODIN OSIRIS and SMR, and the ESA ENVISAT MIPAS, GOMOS and SCIAMACHY. The objective was to evaluate their respective performances (altitude registration, precision and accuracy) in the tropical UT/LS by comparison with the many profiles of the balloon flights.

6.8.1 Ozone

Based on the finding that the ozone variability is small (<2%) in the tropical stratosphere above 19 km, an original statistical approach has been developed for the evaluation of satellite retrievals consisting of comparing zonal mean profiles indicative of biases in altitude registration and systematic errors, and variability (standard deviation compared to the mean), indicative of the random error of each instrument (Borchi et al., 2005, Borchi et al., same issue). Using this technique, the performances of all satellite ozone profile measurements in the tropics available during the MIR flight periods have been investigated by comparison with this data set. Systematic altitude shifts could be observed in satellite profiles, varying from <50 m for the GOMOS stellar occultation instrument, followed by +100/200 m for solar occultation systems (SAGE II, HALOE above 22 km), but as large as –900 m for the OSIRIS limb viewing system. The ozone relative biases are generally limited, between –4% and +4%, for measurements in the visible Chappuis bands (SAGE II and III, GOMOS above 22 km and OSIRIS), the near IR (HALOE above 22 km) and the ozonesondes, but increase to +5.5% in the UV (SCIAMACHY), and +7% in the mid-IR (MIPAS) and the submillimetric range (ODIN-SMR). Regarding precision, evaluated statistically from the zonal variability of ozone concentration, the best measurements are found to be those of SAGE II (2%), followed by HALOE above 22 km (3–4%), ozonesondes, SAGE III and OSIRIS and SCIAMACHY (~5%), GOMOS above 22 km, MIPAS (8.5%) and finally SMR (16%). Overall, satellite ozone measurements appear little reliable in the tropical troposphere, except those of SAGE II (and eventually SAGE III), though low biased by 50% and of limited precision.

6.8.2 Bromine oxide

The bromine oxide profiles observed by the SAOZ UV extended version in the tropics in 2003 and 2004 have been used together with other measurements performed by the same instrument and others at mid-and high altitude, to validate the BrO profile retrievals from the limb observations of SCIAMACHY– ENVISAT at the Harvard Smithsonian Center for Astrophysics (Sioris et al., 2006) and at the University of Heidelberg (Dorf et al., 2006). Overall, after compensation of the BrO photochemical change between the local time of the SCIAMACHY overpass around 10:30 LT and that of the balloon flights in late afternoon, using a photochemical model, satellite-retrieved profiles are found to be consistent with those of the balloons within ±20%,.

6.8.3 Nitrous oxide

On 18 February 2003, the DIRAC gas chromatograph was flown from Bauru (pre-HIBISCUS 2003 campaign) in whole air sampling mode (no adsorbent trap). This enabled a vertical profile of N_2O to be measured. The N_2O profile has since been used as part of the Odin/SMR satellite validation for which N_2O is a target gas (Urban et al., 2005). The N_2O profiles were within instrument uncertainties over all altitudes available for comparison, with the exception of the 23 to 26 km region, where the DIRAC N_2O observations were significantly lower than those from Odin/SMR. The difference was ascribed to horizontal variability in the Bauru region.

6.8.4 Water vapour

The water vapour measurements of GOMOS, SAOZ-MIR, MIPAS, HALOE, SAGE II and AIRS between 11–26 km in the UT/LS have been compared using the statistical method of zonal mean profiles and variability developed for ozone (Montoux et al., 2007[10]). Above 20 km in the stratosphere, all measurements were found to be consistent within ±20% compared to AIRS, AIRS, SAOZ and GOMOS being wetter than others at 25 km. Their precision evaluated from the variability, decreases from 5–10% for HALOE, MIPAS and SAGE II, to 20% for GOMOS and SAOZ and 35% for AIRS.

In the upper troposphere, the difference with AIRS increases to within ±20–30% with the exception of HALOE found to be dry biased by 60% compared to all others. At these levels, their variability, largely due to the atmosphere, is of the order of ±50% on average, except for MIPAS (>100%) suggesting a fast increase of random error of this instrument below 20 km.

As for ozone, those results demonstrate the quality of satellite remote water vapour measurements in the stratosphere, but also the difficulty of getting precise information below 20 km in the Tropical Tropopause Layer.

7 Summary

It is obvious from the HIBISCUS project that the mechanisms involved in the troposphere-stratosphere exchange in the tropics are far from being fully understood. The main reason for that is the deficiency of data in a region, which could generally not be observed reliably from space and of too high altitude for being studied with conventional aircraft. A significant amount of progress has been achieved within the project relevant to the clarification of the mechanisms involved in TTL dynamics, microphysics and chemistry and their implications for the stratosphere.

Overall, the composition of the Tropical Tropopause Layer, the region between 14 and 19 km of intermediate lapse rate between the almost adiabatic upper tropo-

[10]Montoux, N., Hauchecorne, A., Pommereau, J.-P., Durry, G., Morel, B., Jones, R. L., Lefèvre, F., and Bencherif, H.: Comparison of balloon and satellite water vapour profiles obtained in the southern tropical UTLS during the HIBISCUS campaign, Atmos. Chem. Phys. Discuss., in preparation, 2007.

sphere and the stable stratosphere, appears highly variable. Tracers and ozone measurements performed at both the local and the global scale indicate a strong quasi-horizontal isentropic exchange with the lowermost mid-latitude stratosphere suggesting that the barrier associated to the tropical jet is highly permeable in the summer at these levels. But the project also provides clear indications of strong episodic updraught of cold air, short-lived tracers, low ozone, humidity and ice particles across the lapse rate tropopause at about 15 km, up to 18 or 19 km at 420–440 K potential levels in the lower stratosphere, suggesting that, in contrast to oceanic convection penetrating little into the stratosphere, fast daytime developing land convective systems could be a major mechanism in the troposphere-stratosphere exchange at the global scale.

The data also show that two important species, NO_x and water vapour, behave differently. As seen from the NO_2 concentration measurements on zonal scales, large NO_x production by lightning is observed, peaking at 12–14 km in the upper troposphere, principally over land convective areas where thunderstorms are developing in the afternoon and vanishing overnight, in contrast to the low diurnal variation in oceanic convection where lighting is rare.

Regarding water vapour, strong humidity uplifts across the lapse rate tropopause have definitely been observed over deep convective cells. On average, the zonal survey during the austral summer shows a minimum mixing ratio, the hygropause, at about 18 km at or little above the cold point, varying from 3 to 5 ppm, wetter above land, as well as oceanic convergence zones where the temperature of the cold point is the coldest, than over warmer oceanic subsident areas. These findings are consistent with the MLS/UARS observations from space at 100 hPa around 20° S in the austral summer of 1992, showing 5 ppm maxima over Africa, South America and the West Pacific. No dehydration could be observed either locally or zonally, which could be explained by the significantly warmer temperature of the TTL at the latitude of the HIBISCUS observations, compared to the equatorial Micronesian warm pool. However, the vertical, longitudinal and latitudinal distributions of water vapour provided by the ECMWF-REPROBUS model differ significantly from these observations. The resolu-

tion of these contradictions will require obviously further efforts, but it is already clear that the HIBISCUS picture of water distribution in the TTL differs significantly from that currently accepted.

Cirrus clouds have also been observed at both local and global scale showing a maximum frequency over convective zones, in agreement with previous reports from SAGE 2, but limited to the altitude of the lapse rate tropopause at 15 km or below. Nothing could be observed higher at the altitude of the cold point, except the sporadic presence of particles up to 19 km. The formation of cirrus clouds at 14–15 km could be successfully captured by a microphysical model, although the particles are currently still too large and too few.

Overall, the HIBISCUS project has resulted in new information on the TTL over a land convergence zone, a situation that has previously been the subject of very little exploration. A number of intriguing observations have been obtained which are described and analysed in the specific papers of this special issue.

Acknowledgements. The authors thank the coordinators of TroCCiBras for providing the infrastructure to host HIBISCUS, and the personnel of the Meteorological Research Institute (IPMet) of the São Paulo State University (UNESP), including the students from the Federal University of Rio de Janeiro (UFRJ) and the Center of Laser Applications (CLA) of the University of São Paulo (USP) and J. L. Gomes of the Center for Weather Forecast and Climatic Studies (CPTEC), as well as the staff of the Centre National d'Etudes Spatiales (CNES) for their support with weather briefing, balloon, radar, lidar and radiosondes operations, F. Posny and S. Oltmans for the ozonesondes ascents performed during the MIR overpasses above Reunion Island, Samoa and Fidji. ECMWF and NCAR/NCEP are thanked for supplying meteorological data. The HIBISCUS project was supported by the European Commission (contract EVK2-2001-000111), the ENVISAT validation programme of the European Space Agency (project 713), the Programme National de Chimie de l'Atmosphère (PNCA) and the Centre National d'Etudes Spatiales (CNES) in France, the Natural Environment Research Council (NERC) in the UK. Computer resources for BRAMS mesoscale modelling were provided by CINES (Centre Informatique National de l'Enseignement Supérieur, project 2227). They are all gratefully acknowledged.

References

Alcala, C. M. and Dessler, A. E.: Observations of deep convection in the tropics using the Tropical Rainfall Measuring Mission (TRMM) precipitation radar, J. Geophys. Res., 107(D24), 4792, doi:10.1029/2002/D002457, 2002

Adriani, A., Cairo, F., Pulvurenti, L., Cardillo, C., Viterbini, M., Di Francesco, G., and Pommereau, J. P.: Aerosol and polar stratospheric clouds observations by laser backscattersonde in the frame of the European project Stratospheric Regular Soundings, Ann. Geophys., 17, 1352–1360, 1999, http://www.ann-geophys.net/17/1352/1999/.

Borchi, F., Pommereau, J.-P., Garnier, A., and Pinharanda, M.: Evaluation of SHADOZ sondes, HALOE and SAGE II ozone profiles at the tropics from SAOZ UV-Vis remote measurements onboard long duration balloons, Atmos. Chem. Phys., 5, 1381–1397, 2005, http://www.atmos-chem-phys.net/5/1381/2005/.

Borchi, F. and Pommereau, J.-P.: Evaluation of ozonesondes, HALOE, SAGE II and III, Odin-OSIRIS and SMR, and ENVISAT-GOMOS, -SCIAMACHY and -MIPAS ozone profiles in the tropics from SAOZ long duration balloon measurements in 2003 and 2004, Atmos. Chem. Phys. Discuss., 6, 10 087–10 152. 2006.

Buontempo, C., Cairo, F., Di Donfrancesco, G., Morbidini, R., Viterbini, M., and Adriani, A.: Optical measurements of atmospheric particles from airborne platform: in-situ and remote sensing instruments for balloons and aircrafts, Ann. Geophys., 49, 57–64, 2006, http://www.ann-geophys.net/49/57/2006/.

Bradshaw, N. G., Vaughan, G., Busen, R., Garcelon, S., Jones, R. L., Gardiner, T., and Hacker, J.: Tracer filamentation generated by small scale Rossby wave breaking in the lower stratosphere, J. Geophys. Res., 107, 4689, doi:10.1029/2001JD000432.2002.

Brewer, A. W.: Evidence for a world circulation provided by the measurements of helium and water vapour distribution in the stratosphere, Q. J. R. Meteorol. Soc., 75, 351–363, 1949.

Danielsen, E. F.: A dehydration mechanism for the stratosphere, Geophys. Res. Lett., 9, 605–608, 1982.

Danielsen E. F: In situ evidence of rapid, vertical, irreversible transport of lower tropospheric air into the lower stratospehre by convective cloud turrets and by large scale upwelling in tropical cyclones, J. Geophys. Res, 98, 8665-8681, 1993.

Danis, F., Harris, N. R. P., Taylor, W. H., McIntyre, J. D., Simmonds, P .G., and Pyle, J. A.:

DESCARTES: A novel lightweight balloon-borne instrument for measurement of halocarbons, Rev. Sci. Instr., 70, 271–280, 2000.

Dessler, A. E.: A reexamination of the “stratospheric fountain” hypothesis, Geophys. Res. Lett., 25, 4165–4168, 1998.

Di Donfrancesco, G., Cairo, F., Viterbini, M., Morbidini, R., Buontempo, C., Fierli, F., Cardillo, F., Snels, M., Liberti, G. L., and Di Paola, F.: Cloud and aerosol detection by a balloon-borne lidars and backscattersondes in the UTLS during the HIBISCUS campaign: optical and dynamical Properties, Geophys. Res. Abstracts, 7, 03355, 2005a.

Di Donfrancesco, G., Cairo, F., Held, G., and Fierli, F.: Contemporary Measurements of a Ground-based Weather Radar and a Balloon-borne Lidar at Bauru during the HIBISCUS Campaign: A Powerful Synergy in Cloud Physics Studies, 32nd Conference on Radar Meteorology, AMS, Albuquerque, New Mexico, 24–29, 2005b.

Di Donfrancesco, G., Cairo, F., Buontempo, C., Adriani, A., Viterbini, M., Snels, M., Morbidini, R., Piccolo, F., Cardillo, F., Pommereau, J.-P., and Garnier, A.: Balloon borne lidar for cloud physics studies, Appl. Opt., 45, 5701–5708, 2006

Dorf, M., Bosch, H., Butz, A., Camy-Peyret, C., Chipperfield, M., Engel, A., Goutail, F., Grunow, K., Hendrick, F., Hrechanyy, S., Naujokat, B., Pommereau, J.-P., van Roozendael, M., Sioris, C., Stroh, F., Weldner, F., and Pfeilsticker, K.: Balloon-borne stratospheric BrO measurments : comparison with Envisat/Sciamachy BrO limb measurements, Atmos. Chem. Phys., 6, 2483–2501, 2005, http://www.atmos-chem-phys.net/6/2483/2005/.

Durry, G., Amarouche, N., Zéninari, V., Parvitte, B., Lebarbu, T., and Ovarlez, J.: In situ sensing of the middle atmosphere with balloonborne near-infrared laser diodes, Spectrochimica Acta A, 60(14), 3371–3379, 2004.

Durry, G., Huret, N., Hauchecorne, A., Marecal, V., Pommereau, J-P. Jones, R., Held, G., Larsen, N., and Renard, J.-B.: Isentropic advection and convective lifting of water vapor in the UT – LS as observed over Brazil (22° S) in February 2004 by in situ high-resolution measurements of H_2O, CH_4, O_3 and temperature, Atmos. Chem. Phys. Discuss., 6, 12 469–12 501, 2006.

Folkins, I., Loewenstein, M., Podolske, J., Oltmans, S. J., and Profitt, M.: A barrier to vertical mixing at 14 km in the tropicas: Evidence from ozonesondes and aircraft measurements, J. Geophys. Res., 104, 22 095–22 102, 1999.

Freitas, S. R., Silva Dias, M. A. F., Silva Dias, P. L., Longo, K. M., Artaxo, P., Andreae, M. O,

and Fischer, H.: A convective kinematic trajectory technique for low-resolution atmospheric models, J. Geophys. Res., 105(D19), 24 375–24 386, 2000.
Garnier, A., Pommereau, J.-P., Cocquerez, P., Held G., and the HIBISCUS partners: The balloon flights in the Tropics of the HIBISCUS project, Proc. 17th ESA Symp. Europ. on Rocket & Balloon programmes, ESA SP-590, 203–208, 2005.
Gettelman A., Salby, M. L., and Sassi, F.: Distribution and influence of convection in the tropical tropopause region, J. Geophys. Res., 107(D10), 4080, doi:10.1029/2001JD001048, 2002.
Gettelman A., Forster P. M. D., Fujiwara M., Fu, Q., Vomel, H., Gohar, L. K., Johanson, C., and Ammerman, M.: Radiation balance of the tropical tropopause layer, J. Geophys. Res., 109(D7), doi:10.1029/2003JD004190, 2004.
Gomes, A. M. and Held, G.: Determinação e avaliação do parâmetro densidade VIL para alerta de tempestades. Proc. XIII Congresso Brasileiro de Meteorologia, (CD ROM), Sociedade Brasileira de Meteorologia, 12pp, 2004.
Hansford, G. M, Freshwater, R. A., Bosch, R. A., Cox, R. A., Jones, R. L., Pratt, K. F. E., and Williams, D. E.: A Low Cost Instrument based on a Solid State Sensor for Balloon-borne Atmospheric O_3 Profile Sounding, J. Environ. Monit., 7, 158–162 2005.
Hansford, G. M., Freshwater, R. A., Eden, L., Turnbull, K. F. V., Hadaway, D. E., Ostanin, V. P., and Jones, R. L.: A lightweight dew-/frost-point hygrometer based on a surface acoustic wave sensor for balloon-borne atmospheric water vapour profile sounding, Rev. Sci. Instr, 77, 014502, 2006
Hauchecorne, A., Godin, S., Marchand, M., Heese, B., and Souprayen, C.: Quantification of the Transport of Chemical Constituents from the Polar Vortex to Middle Latitudes in the Lower Stratosphere using the High-Resolution Advection Model MIMOSA and Effective Diffusivity, J. Geophys. Res., 107, 8289, doi:10.129/2001JD000491, 2002.
Held, G., Gomes, A. M., and Figueiredo, J. C.: Statistics of echo top and VIL density and local synoptic situations in São Paulo State, Proc. TROPIC Workshop, Wessling, 14-16 May 2003 (http://www.ipmet.unesp.br/troccibras – "Publications"), 2003.
Held, G. (Ed.): Proc. HIBISCUS/TroCCiBras/TROCINO$_X$ Workshop, 32pp, http://www.ipmet.unesp.br/troccibras, 2004.
Held, G., Calheiros, R. V., Pommereau, J.-P., and Gomes, A. M.: A preview of preliminary results from the TroCCiBras, trOCCINO$_X$ and HIBISCUS campaign 2004. Proc. XIII Congresso Brasileiro de Meteorologia, (CD ROM), Sociedade Brasileira de Meteorologia, 15pp, 2004a.
Held, G., Calheiros, R. V., Schlager, H., Pommereau, J.-P., and Morimoto, T.: TroCCiBras and

its Partner Projects TROCCINO$_X$ and HIBISCUS: Monitoring the Atmosphere from Ground-level to the Lower Stratosphere, Proc. Int. Conf on Grounding and Earthing (GROUND'2004) & 1st Int. Conf on Lightning Physics and Effects, Belo Horizonte, 17–22, 2004b.
Hertzog, A., Basdevant, C., and Vial, F.: An assessment of ECMWF and NCEP/NCAR reanalyses in the southern hemisphere at the end of the pre-satellite era: results from the EOLE experiment (1971–1972), Mon. Wea. Rev., 134, 3367–3383, 2006.
Hoskins, B. J: Towards a PV-θ view of the general circulation, Tellus Ser. A, 43(4), 27–35, 1991
Kistler, R., Kalnay, E., Collins, W., et al.: The NCEP-NCAR 50-year reanalysis: Monthly means CD-ROM and documentation, Bull. Am. Meteorol. Soc., 82, 247–267, 2000.
Knudsen, B. M., Pommereau, J.-P., Garnier, A., Nunes Pinharanda, M., Denis, L., Newman, P. A., Letrenne, G., and Durand, M.: Accuracy of analysed stratospheric temperatures in the winter Arctic vortex from infrared Montgolfier long-duration balloon flights. 2. Results, J. Geophys. Res., 107(D20), 4316, doi:10.129/2001JD001329, 2002.
Knudsen, B. M., Christensen, T., Hertzog, A., Deme, A., Vial, F., and Pommereau, J.-P.: Accuracy of analyzed temperatures, winds and trajectories in the Southern Hemisphere tropical and mid-latitude stratosphere as compared to long-duration balloon flights, Atmos. Chem. Phys., 6, 5391–5397, 2006, http://www.atmos-chem-phys.net/6/5391/2006/.
Kylling, A., Danielsen, T., Blumthaler, M., Schreder, J., and Johnsen, B.: Twilight tropospheric and stratospheric photodissociation rates derived from balloon borne radiation measurements, Atmos. Chem. Phys., 3, 377–385, 2003, http://www.atmos-chem-phys.net/3/377/2003/.
Lefèvre, F., Brasseur, G. P., Folkins, I., Smith, A. K., and Simon, P., Chemistry of the 1991–1992 stratospheric winter: three dimensional model simulations, J. Geophys. Res., 99, 8183–8195, 1994.
Legras, B., Pisso, I., Lefevre, F., and Berthet, G.: Variability of the Lagrangian turbulent diffusion in the lower stratosphere, Atmos. Chem. Phys, 5, 1605–1622, 2005
Levine, J. G., Braesicke, P., Harris, N. R. P., Savage N. H., and Pyle, J. A.: Pathways and Timescales for Troposphere-to Stratosphere Transport via the Tropical Tropopause Layer and their Relevance for Very Short Lived Substances, J. Geophys. Res., 112, doi:10.129/2005JD006940, 2007.
Liu, C. and Zipser, E. J.: Global distribution of convection penetrating the tropical tropopause, J. Geophys. Res., 110, D23104, doi:10.1029/2005JD006063, 2005.

Marécal, V., Rivière, E., Held, G., Cautenet, S., and Freitas, S.: Modelling study of the impact of deep convection on the UTLS air composition. Part I: analysis of ozone precursors, Atmos. Chem. Phys., 6, 1567–1584, 2006, http://www.atmos-chem-phys.net/6/1567/2006/.

Marécal, V., Durry, G., Longo, K., Freitas, S., Rivière, E. D., and Pirre, M.: Mesoscale modelling of water vapour in the tropical UTLS: two case studies of the HIBISCUS campaign, Atmos. Chem. Phys. Discuss., 6, 8241–8284, 2006, http://www.atmos-chem-phys-discuss.net/6/8241/2006/.

Mayer, B. and Kylling, A.: Technical note: The libRadtran software package for radiative transfer calculations – description and example of use, Atmos. Chem. Phys., 5, 1855–1877, 2005, http://www.atmos-chem-phys.net/5/1855/2005/.

Newman, P. A., Harris, N. R. P., Adriani, A., Amanatidis, G., Anderson, J., Braathen, G., Brune, W., Carslaw, K., Craig, M., DeCola, P., Guirlet, M., Hipskind, S., Kurylo, M., Küllmann, Larsen, N., Mégie, G., Pommereau, J.-P., Lamont Poole, H., Schoeberl, M., Stroh, F., Toon, B., Trepte, C., and van Roozendael, M.: An overview of the SOLVE-THESEO 2000 campaign, J. Geophys. Res., 107(D20), 8259, doi:10.129/2001JD001303, 2002.

Newell, R. E. and Gould-Stewart, S.: A stratospheric fountain?, J. Atmos. Sci., 38, 2789–2796, 1981.

Nielsen, J. K., Larsen, N., Cairo, F., Di Donfrancesco, G., Rosen, J. M., Durry, G., Hels, G., and Pommereau, J.-P.: Solid particles in the tropical lower stratosphere, Atmos. Chem. Phys., 7, 685–695, 2007, http://www.atmos-chem-phys.net/7/685/2007/.

O'Connor, F. M., Carver, G. D., Savage, N. H., Pyle, J. A., Methven, J., Arnold, S. R., Dewey, K., and Kent, K.: Comparison and visualisation of high-resolution transport modeling with aircraft measurements, Atmos. Sci. Lett., 6, 164–170, doi:10.1002/asl.111, 2005.

Pfister, L., Selkirk, H. B., Jensen, E. J., Schoeberl, M. R., Toon, B., Browell, E. V., Grant, W. B., Gary, B., Mahonney, M. J., Bui, T. V., and Hintsa, E.: Aircraft observations of thin cirrus clouds near the tropical tropopause, J. Geophys. Res., 106, 9765–9786, 2001.

Pielke, R. A., Cotton, W. R., Walko, R. L., Tremback, C. J., Lyons, W. A., Grasso, L. D., Nicholls, M. E., Moran, M. D., Wesley, D. A., Lee T. J., and Copeland, J. H.: A comprehensive meteorological modelling system-RAMS, Meteorol. Atmos., 49, 69–91, 1992.

Pommereau, J.-P. and Piquard, J.: Ozone, Nitrogen dioxide and Aerosol vertical distributions by UV-visible solar occultation from balloons, Geophys. Res. Lett, 21, 1227–1230, 1994.

Pommereau, J.-P., Goutail, F., Pundt, I., Pyle, J. A., Danis, F., Hansford, G., Freshwater, R. A., Robinson, A., Jones, R. L., Harris, N. R. P., Adriani, A., Cairo, F., Pulvurenti, L., Difrancesco, G., Kirkwood, S., Nilson, H., Arvelius, J., Woods, P., Swann, N. R., Howeison, H., Garcelon, S., Gardiner, T., Deshler T., and Buivan, A.: Small balloons for stratospheric ozone research and satellite validation, Proc. 14th ESA Symp. on European Rocket and Balloon programmes, ESA, SP-437, 609–614, 1999.

Pommereau, J.-P., Garnier, A., Nunes Pinharanda, M., Borchi, F., Hauchecorne, A., and Letrenne, G.: Long Duration SAOZ Infra-Red Montgolfier flights at the Tropics for the validation of ozone measuring satellites, Proc. 16th ESA Symp. on European Rocket and Balloon Programmes, ESA SP-530, 445–450, 2003.

Prather, M. J.: Numerical advection by conservation of second-order moments, J. Geophys. Res., 91, 6671–6681, 1986

Pundt, I. Pommereau, J.-P., Chipperfield, M. P., van Roozendael, M., and Goutail, F.: Climatology of the stratospheric BrO vertical distribution by balloon-borne UV-Vis spectrometry, J. Geophys. Res., 107(D24), 4806, doi:10.1029/2002JD002230, 2002.

Rabier, F., Järvinen, H., Klinker, E., Mahfouf, J.-F., and Simmons, A.: The ECMWF operational implementation of four dimensional variation assimilation. I: Experimental results with simplified physics, Q. J. R. Meteorol. Soc., 126, 1143–1170, 2000.

Rivière, E. D., Pirre, M., Berthet, G., Renard, J.-B. , Taupin, F.G., Huret, N., Chartier, M., Knudsen, B. M., and Lefèvre, F.: On the interaction between Nitrogen and Halogen species in the arctic polar vortex during THESEO and THESEO 2000, J. Geophys. Res., 108(D5), 8311, doi:10.1029/2002JD002087, 2003.

Rivière, E. D, V. Marécal, Larsen, N., and Cautenet, S.: Modelling study of the impact of deep convection on the UTLS air composition, Part II: Ozone budget in the TTL, Atmos. Chem. Phys., 6, 1585-1598, 2006, http://www.atmos-chem-phys.net/6/1585/2006/.

Robinson, A. D., McIntyre, J., Harris, N. R. P., Pyle, J. A., Simmonds, P. G., and Danis, F.: A lightweight balloon-borne gas chromatograph for in situ measurements of atmospheric halocarbons, Rev. Sci. Instr., 71, 4553–4560, 2000.

Sherwood, S. C. and Dessler, A. E.: On the control of stratospheric humidity, Geophys. Res. Lett., 2513–2516, 2000.

Rosen, J. M. and Kjome, N. T.: Backscattersonde – A new instrument for atmospheric aerosol research, Appl. Opt., 30, 1552–1561, 1991.

Simmons, A. J. and Gibson, J. K.: The ERA-40 project plan, ERA-40 project report series No.1, European Centre for Medium-Range Weather Forecasts, Reading, UK, 2000.

Shutts, G. J. and Gray, M.: A numerical modelling study of the geostrophic adjustment process following deep convection, Q. J. R. Meteorol. Soc., 126, 823–863, 1994

Sioris, C. E. , Kovalenko, L. J., McLinden, C. A., Salawitch, R. J., van Roozendael, M., Goutail, F., Dorf, M., Pfeilsticker, K., Chance, K., von Savigny, C., Camy-Peyret, C., Payan, S., Liu, X., Kurosu, T. P., Pommereau, J.-P., Bösch, H., and Frerick, J.: Latitudinal and vertical distribution of bromine moNO_xide and inorganic bromine in the lower stratosphere from SCIAMACHY limb scatter measurements, J. Geophys. Res., 111, D14301, doi:10.1029/2005JD006479, 2006.

Suomi, V. E. and Kuhn, P. M.: An economical net radiometer, Tellus, 10, 161–163, 1958.

Swann, H. A.: The development and validation of a microphysics scheme for cloud resolving model simulations of deep convection. PhD thesis, University of Reading, 1996.

Swann, H. A.: Sensitivity to the representation of precipitating ice in CRM simulations of deep convection, Atm. Res., 47, 415–435, 1998.

Tiedke, M.: A comprehensive mass flux scheme for cumulus parameterization in large-scale models, Mon. Weather Rev., 117, 1779–1800, 1989.

Urban, J., Lautie, N., Le Flochmoen, E., Jimenez, C., Eriksson, P., de La Noe, J., Dupuy, E., El Amraoui, L., Frisk, U., Jegou, F., Murtagh, D., Olberg, M., Ricaud, P., Camy-Peyret, C., Dufour, G., Payan, S., Huret, N., Pirre, M., Robinson, A. D., Harris, N. R. P., Bremer, H., Kleinbohl, A., Kullmann, K., Kunzi, K., Kuttippurath, J., Ejiri, M., Nakajima, H., Sasano, Y., Sugita, T., Yokota, T., Piccolo, T., Raspollini P., and Ridolfi, M.: Odin/SMR Limb Observations of Stratospheric Trace Gases: Validation of N_2O, J. Geophys. Res., 110, D09301, doi:10.1029/2004JD005394, 2005.

van Aalst, M. K., van den Broek, M. M. P., Bregman, A., Bruhl, C., Steil, B., Toon, G. C., Garcelon, S., Hansford, G. M., Jones, R. L., Gardiner, T. D., Roelofs, G. J., Lelieveld, J., and Crutzen, P. J.: Trace gas transport in the 1999/2000 Arctic winter: comparison of nudged GCM runs with observations, Atmos. Chem. Phys., 4, 81–93, 2004, http://www.atmos-chem-phys.net/4/81/2004/.

Table 1. Instrumentation of short-duration balloons during the Pre-HIBISCUS campaign in 2003.

Instrument (Institute)	Parameter	ZL1	SF	ZL2
SAOZ Vis, SA	O_3, NO_2 profiles	X		X
SAOZ UV, SA	BrO profile			X
SAOZ H_2O, SA	H_2O profile	X		
DESCARTES, UCAM	Halogen compounds		X	
DIRAC GC,UCAM	N_2O	X		X
DIRAC, GC UCAM	Halogen compounds		X	
SAW Hygrometer, UCA	H_2O	X	X	X
SSS Ozone sensor, UCAM	O_3	X	X	X
Micro-lidar, ENEA/ISAC	Backscatter ratio/polar		X	X

Table 2. Instrumentation of short-duration balloons and number of sondes (Son) during HIBISCUS.

Instrument (Institute)	Parameter	ZL1	ZL2	SF1	SF2	SF3	SF4	Son
SAOZ Vis, SA	O_3, NO_2 profiles	X	X					
SAOZ UV, SA	BrO profile	X	X					
DESCARTES, UCAM	Halogen compounds			X	X	X		
DIRAC GC,UCAM	Halogen compounds	X					X	
Micro DIRAC, UCAM	Test instrument, CFC11			X	X	X		
Micro-SDLA, CNRS	H_2O, CH_4, CO_2				X		X	
TDLAS, NPL	H_2O			X		X		
SAW Hygrometer, UCAM	H_2O			X	X	X	X	
SSS Ozone sensor, UCAM	O_3			X	X	X	X	
Micro-lidar, ENEA/ISAC	Backscatter ratio/polar				X		X	
LABS, ISAC	Backscatter ratio/polar		X	X		X		
BKS sonde DMI, U. Wyo	Backscatter ratio in situ			X				10
Optical Counter, UMIST	Aerosol size distribution							
ECC Ozone, DMI SA	O_3							13
NILUCUBE, NILU	UV-Vis radiation							2
AIRS, CNRS CETP	Electric field, conductivity			X		X		

Table 3. Dates and type of sondes (BKS: backscatter; O_3: ECC ozonesonde; Nilucube).

Date UT time	Instruments	Comments
10 Feb 00:59	BKS, O_3	28.5 km No cirrus
11 Feb 23:57	BKS, O_3	28.0 km Thin cloud layer at 9–10 km
13 Feb 13:00	NILUCUBE	20 km. Clear sky. Bright low alt cumulus
13 Feb 22:35	BKS, O_3	SF2, 26.9 km, Thin cirrus up to 13 km ≈ app. 2 km below bottom of TTL
16 Feb 00:07	BKS, O_3	28.4 km. No cirrus
17 Feb 00:05	BKS, O_3	SF1. 26.9 km. No cirrus
19 Feb 00 :07	BKS, O_3	27.7 km. Very thin cirrus up to 14 km
20 Feb 15:35	O_3	33 km
20 Feb 23:58	BKS, O_3	25.4 km. Thick (2–3 km) cirrus up to bottom of TTL at 14.4 km. Unusual aerosol layer at 16.5–18 km only seen on descent. Close to local thunderstorms.
21 Feb 22:24	BKS, O_3	33.2 km. Very thin cirrus layer at the bottom of the TTL at 15 km, only seen on descent. Launched close to local thunderstorms.
23 Feb 22:41	BKS, O_3	26.1 km (O_3 unreliable above 22.6 km). Thick cloud layer up to 13 km. Launched downwind of convective systems.
24 Feb 22:30	BKS, O_3	SF4. 28.7 km. Very thin cirrus layers up to 15 km. Thick cloud layer up to 14 km. Launched downwind of convective systems. Depolarisation data.
25 Feb 15:00	NILUCUBE	20 km. Overcast conditions by high altitude cirrus
26 Feb 23:35	O_3	SF3. 30.1 km.
6 March 23:00	O_3	31.7 km

Table 4. Diameter, instrumentation, date of launch and duration of SPBs.

Balloon	Instrument	Start	Dur.	Comments
BP1 10 m	Met, turbulence LMD	6 Feb	13 d	Telemetry failed after few hours
BP2 8.5 m	Met, O_3/H_2O UCAM	12 Feb	1 d	No SSS/SAW data after 14 d
BP3 10m	Met, turbulence LMD	12 Feb	53 d	No SSS/SAW data after 3 d
BP4 8.5 m	Met sensors	29 Feb	80 d	No turbulence data after 7 d
BP5 10 m	Met, O_3/H_2O UCAM	6 March	39 d	
BP6 8.5 m	Met, turbulence LMD	7 March	56 d	
BP7 10 m	Met, O_3/H_2O UCAM	9 March	27 d	
BP8 10 m	Met sensors	11 March	37 d	

Table 5. Instrumentation and duration of IR Montgolfier flights.

Flight	Instrument	Date	Dur	Comments
MIR1	SAOZ spectrometer, O_3, NO_2, H_2O,	4 Feb	9 d	SAOZ detector malfunction
MIR3	Atm. extinct., IR rad, met sensors	26 Feb	39 d	End above tropical storm
MIR2	SAOZ spectrometer, O_3, NO_2, H_2O,	10 March	7 d	End above thunderstorm
	atmos. extinct., IR rad, met sensors			Noise in μlidar,
	lightning detector			40% profiles recoverable
	Micro-lidar			Dropped above 16 km high
	IR radiometer, met sensors			anvils in the SPCZ

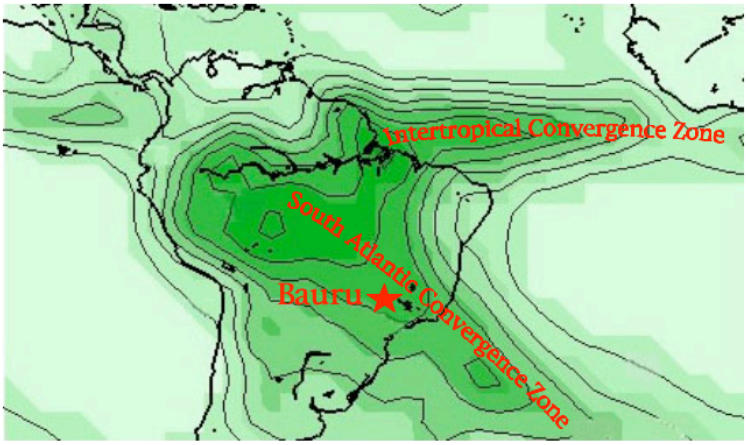

Fig. 1. Rainfall in January. Bauru is located in the convectively active region of the South Atlantic Convergence Zone (SACZ).

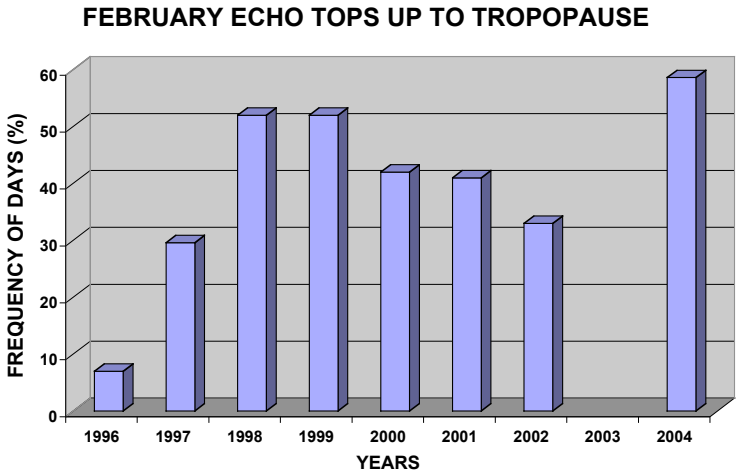

Fig. 2. Frequency of days in February when one or more storm turrets penetrated through the tropopause (Bauru IPMet S-band radar; 240 km range, no survey in 2003).

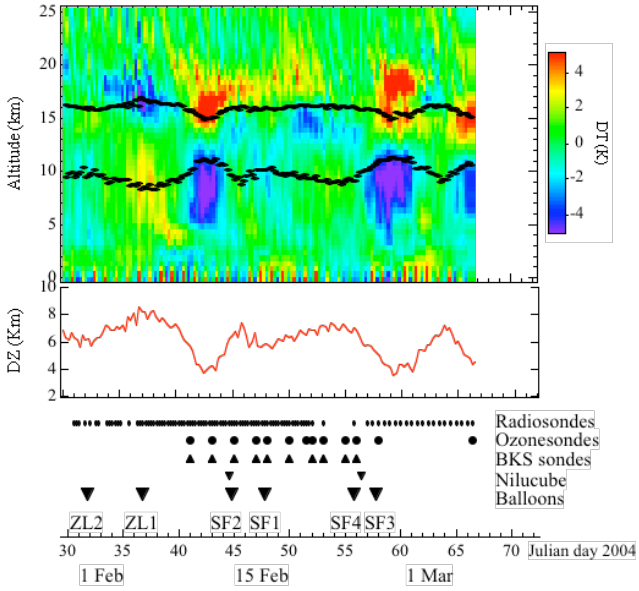

Fig. 3. Timetable of balloon and sonde flights, as well as meteorological conditions in which they took place. Top: 6-hourly ECMWF temperature deviation compared to campaign average profile. Black markers show the altitude of the 340 K and 370 K potential temperature surfaces, whose difference, used as a convection index, is shown in the middle panel (red graph). The intensity of convection above Bauru varies with the slow back and forth displacement of the South Atlantic Convergence Zone (SACZ) and the advection of cold front systems from the SW. Highest convection could be observed between 4–8 February (day 35–39) where the troposphere is warmer by 2–4°C compared to the average and the region of the tropopause cooler by 2–5°C, and of medium intensity between day 45–57 and 62–65. Two periods of low convection could be observed from day 41–44 and 53–56 corresponding to the maximum displacement of the SACZ towards the NE.

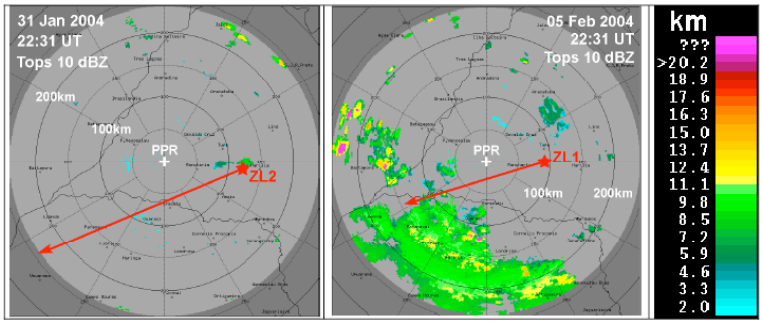

Fig. 4. Echo tops (reflectivity threshold 10 dBZ) seen by the S-Band radar at Presidente Prudente (PPR) during the ZL flights. A star represents the balloon location at the time of the radar image and the tip of the arrow indicates the tangent point. Left: ZL2 at 22:31 UT, 2 h after launch, on 31 January. The IPMet radars of BRU and PPR detected isolated intense storm cells about 200 km north to north-east of the balloon position, topping up to 15 km. Right: ZL1 at sunset at 22:31 UT on 5 February, about 150 min after its launch. The radar image displays a MCS of 300 km extension south to south-west of the flight track, topping at 11–12 km on average, with turrets (red dots) as high as 17–18 km. SAOZ indicates an increase of extinction below 17 km (cirrus), the atmosphere becoming opaque below 16.5 km at sunset in the direction of the sun (arrow).

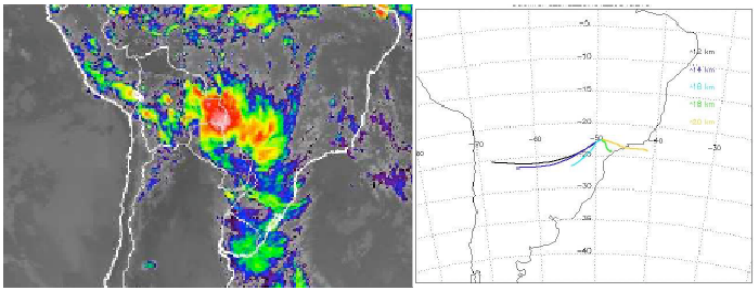

Fig. 5. SF-2 flight on 13 February. Left GOES-E image at 19:15 LT. Right: BRAMS one day 3-D backward trajectories ending at 18:00 UT at 12 km (black), 14 km (blue), 16 km (cyan), 18 km (green) and 20 km (yellow).

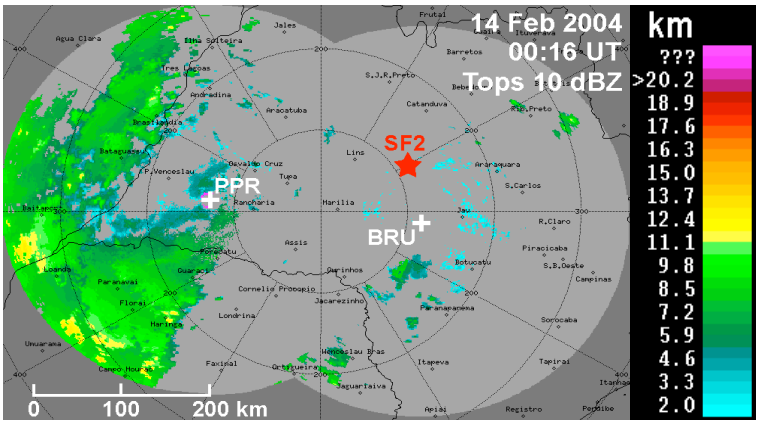

Fig. 6. Echo tops (reflectivity threshold 10 dBZ) observed by the Bauru and Presidente Prudente Radars on 13 February approximately four hours after launch. The SF2 flight location is shown by a star.

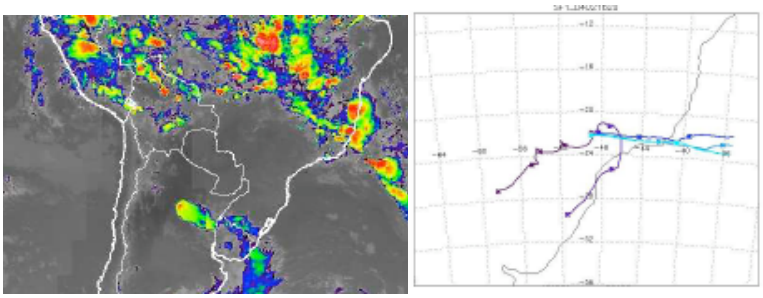

Fig. 7. SF-1 on 16 February. Left: GOES-E image at 19:15 LT. Right BRAMS 4-day backward trajectories at 20:00 LT at 12 km (black), 14 km (blue), 16 km (cyan), 18 km (green) and 20 km (yellow).

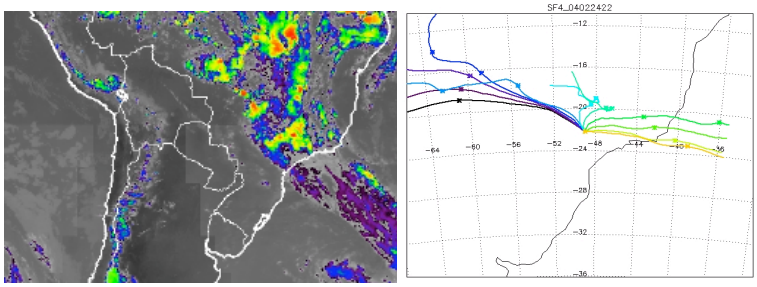

Fig. 8. SF-4 flight on 24 February. Left GOES-E image at 18:15 LT. Right RAMS 5-day backward trajectories at 17:00 LT at 12 km (black), 14 km (blue), 16 km (cyan), 18 km (green) and 20 km (yellow).

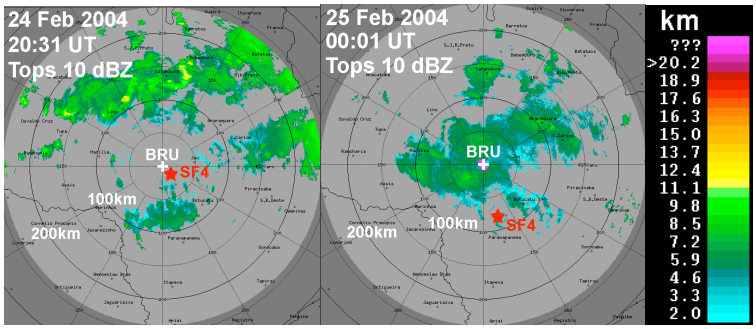

Fig. 9. Echo tops (reflectivity threshold 10 dBZ) seen by the S-Band radar at Bauru (BRU) during the SF4 flight on 24 February 2004. The star represents the balloon location at the time of the radar image. Left: about 30 min after launch; Right: about 4 h after launch, towards the end of its float.

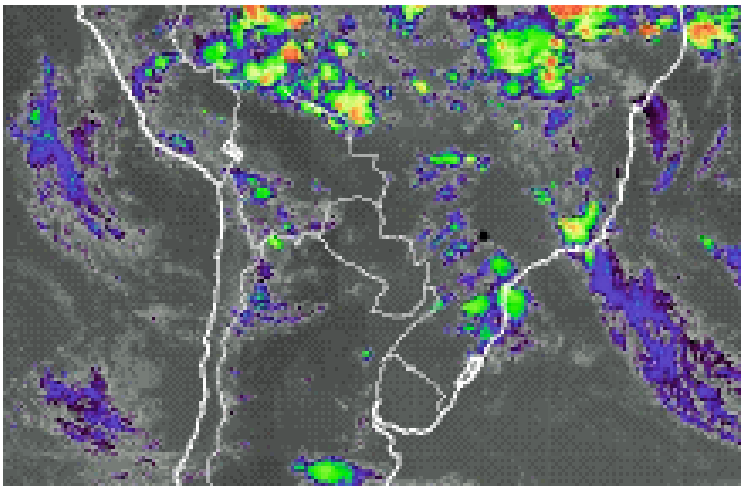

Fig. 10. SF-3 flight on 24 February. GOES-E image at 21:15 LT. Thunderstorms developed over South Brazil in the States of Santa Catarina and Paraná, moving rapidly northwards.

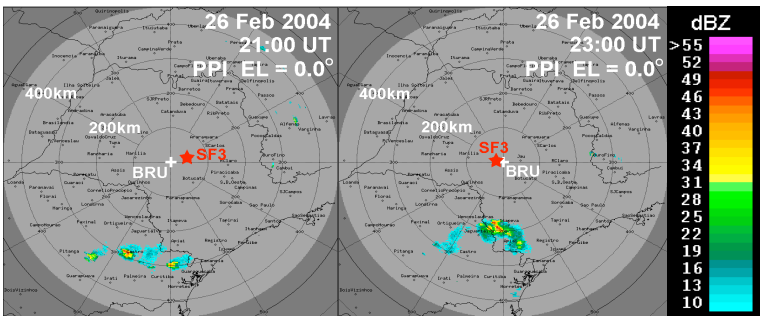

Fig. 11. SF3-flight. Thunderstorms over Paraná approaching from the south, as seen by the Bauru radar at 21:00 and 23:00 UT, respectively; surveillance PPI (450 km range) at 0° elevation. The star represents the SF3 balloon location at the time of the radar image, viz. 1h after launch (left) and during its south-eastwards float (right), respectively.

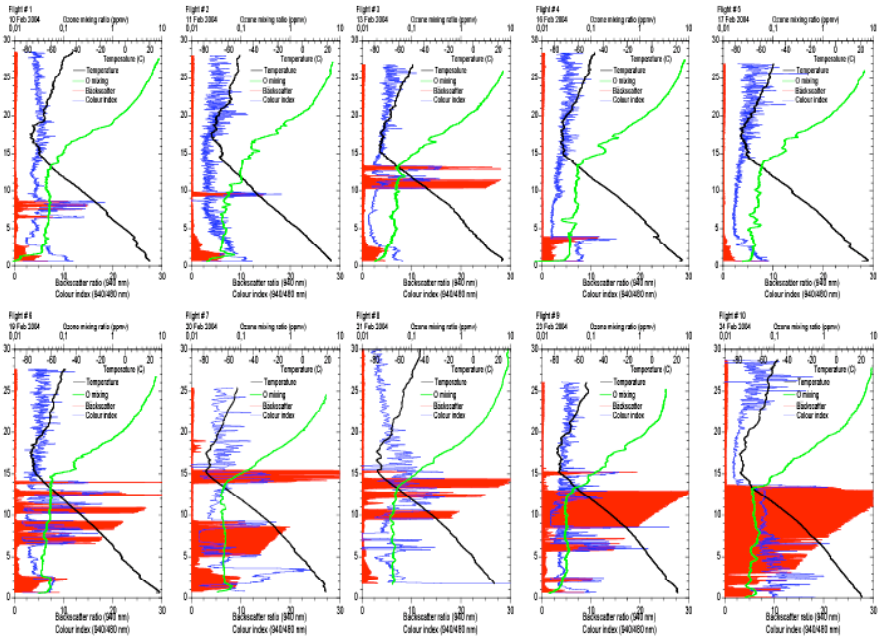

Fig. 12. Ozone mixing ratio (green), backscatter signal (red) and color index (940/460 nm) of the 10 sondes operated by the Danish Meteorological Institutes between 10 and 24 February.

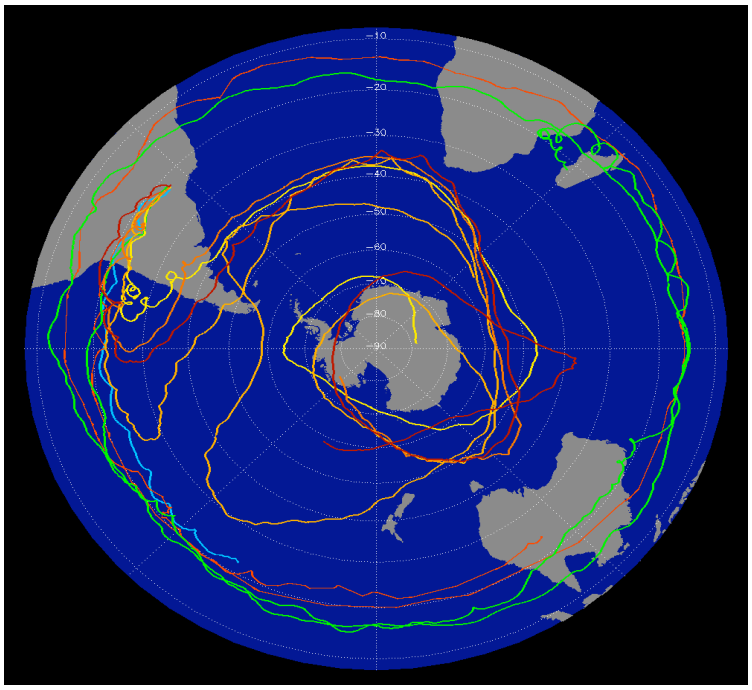

Fig. 13. Trajectories of the 8 SBP. The balloons launched before 12 February remained at tropical latitude, whilst those flown later, after a break of 17 days, were rapidly captured by the mid-latitude westerly flow after crossing the tropical barrier. The loops in the trajectories, particularly in the tropics, are due to inertia gravity waves, which are not well captured by the ECMWF model.

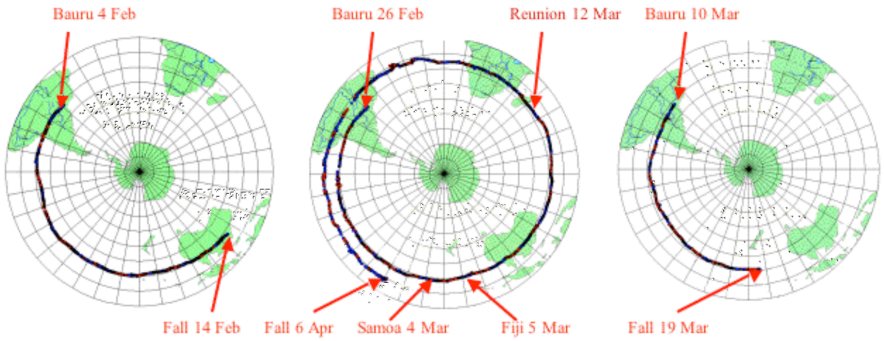

Fig. 14. MIR trajectories. MIR-1 carrying a SAOZ lasted in flight for 9 days before falling in the evening above a tropical storm in NW Australia where it could be recovered. MIR-2 has been flying for 39 days between 20 and 10° S, providing 78 profiles of O_3, NO_2, H_2O and cloud extinction between 6 km or cloud top and 25 km. Collocated ozonesonde ascents have been performed at the SHADOZ stations of Samoa, Fiji and Reunion Island. The flight ended over a thunderstorm in the South Pacific Convergence Zone. Although only of 8-day duration, MIR-3 has allowed to perform promising cloud measurements by the ENEA micro-lidar, flown for the first time on a long-duration balloon, together with the IR global radiometer.

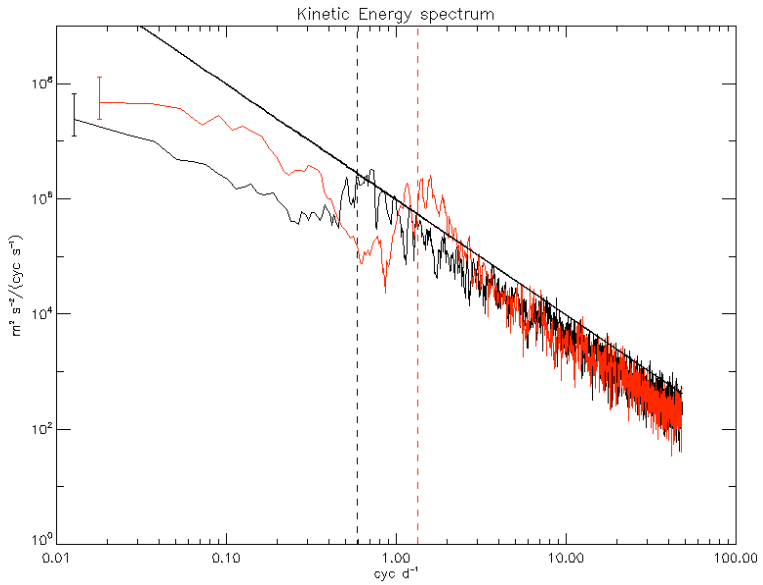

Fig. 15. Horizontal kinetic energy spectra obtained with SPB4 (black) and SPB6 (red) wind observations. The error bars on the left of the spectra show the 90% confidence level. The flight-averaged inertial frequencies are indicated by the vertical dashed lines. A -2 slope (thick black line) is shown for reference.